Overcharging and charge reversal in the electrical double layer around the point of zero charge

G. Iván Guerrero-García, Enrique González-Tovar, Martín Chávez-Páez, and Marcelo Lozada-Cassou

Citation: J. Chem. Phys. **132**, 054903 (2010); doi: 10.1063/1.3294555
View online: http://dx.doi.org/10.1063/1.3294555
View Table of Contents: http://jcp.aip.org/resource/1/JCPSA6/v132/i5
Published by the AIP Publishing LLC.

Overcharging and charge reversal in the electrical double layer around the point of zero charge

G. Iván Guerrero-García,[1,2] Enrique González-Tovar,[1] Martín Chávez-Páez,[1] and Marcelo Lozada-Cassou[2,a)]

[1]*Instituto de Física, Universidad Autónoma de San Luis Potosí, Álvaro Obregón 64, 78000 San Luis Potosí, San Luis Potosí, México*

[2]*Programa de Ingeniería Molecular, Instituto Mexicano del Petróleo, Eje Central Lázaro Cárdenas Norte 152, 07730 México, Distrito Federal, México*

(Received 23 December 2008; accepted 29 December 2009; published online 5 February 2010)

The ionic adsorption around a weakly charged spherical colloid, immersed in size-asymmetric 1:1 and 2:2 salts, is studied. We use the primitive model (PM) of an electrolyte to perform Monte Carlo simulations as well as theoretical calculations by means of the hypernetted chain/mean spherical approximation (HNC/MSA) and the unequal-radius modified Gouy–Chapman (URMGC) integral equations. Structural quantities such as the radial distribution functions, the integrated charge, and the mean electrostatic potential are reported. Our Monte Carlo "experiments" evidence that near the point of zero charge, the smallest ionic species is preferentially adsorbed onto the macroparticle, independently of the sign of the charge carried by this tiniest electrolytic component, giving rise to the appearance of the phenomena of charge reversal (CR) and overcharging (OC). Accordingly, colloidal CR, due to an excessive attachment of counterions, is observed when the macroion is slightly charged and the coions are larger than the counterions. In the opposite situation, i.e., if the counterions are larger than the coions, the central macroion acquires additional like-charge (coions) and hence becomes "overcharged," a feature theoretically predicted in the past [F. Jiménez-Ángeles and M. Lozada-Cassou, J. Phys. Chem. B **108**, 7286 (2004)]. In other words, *here we present the first simulation data on OC in the PM electrical double layer*, showing that close to the point of zero charge, this novel effect surges as a consequence of the ionic size asymmetry. We also find that the HNC/MSA theory captures well the CR and OC phenomena exhibited by the computer experiments, especially as the macroion's charge increases. On the contrary, even if URMGC also displays CR and OC, its predictions do not compare favorably with the Monte Carlo data, evidencing that the inclusion of hard-core correlations in Monte Carlo and HNC/MSA enhances and extends those effects. We explain our findings in terms of the energy-entropy balance. In the field of electrophoresis, it has been generally agreed that the charge of a colloid in motion is partially decreased by counterion adsorption. Depending on the location of the macroion's slipping surface, the OC results of this paper could imply an *increase* in the expected electrophoretic mobility. These observations aware about the interpretation of electrokinetic measurements using the standard Poisson–Boltzmann approximation beyond its validity region. © *2010 American Institute of Physics*. [doi:10.1063/1.3294555]

I. INTRODUCTION

It is widely known in physical chemistry that a surface in contact with an electrolyte solution usually becomes charged and thus that the ions around the interface originate a diffuse structure commonly denoted as the electrical double layer (EDL). One of the most successful early theories used to describe these EDL systems in the dilute and/or weak electrostatic regimes is the classic Poisson–Boltzmann (PB) treatment, which is based on a point-ions representation of an electrolyte.[1,2] Under this approach, it is an admitted fact that the counterions of a binary electrolyte are mostly adsorbed to the electrode when its surface charge density is increased; the coions, on the other hand, are pushed away from the region close to the charged surface.[1–3] As a result, in the PB picture, the main role of the EDL is to neutralize monotonically the surface charge as a function of the distance to the macroparticle, leading to a screened interaction between charged colloids in solution.[4–6] However, starting from the middle of the past century, a number of electrophoretic experiments reported reversed charged particle mobilities, implying that the *effective* charge of a colloid reverses its sign.[7–11] This reversed mobility had been theoretically predicted since 1985 (Refs. 12–14) and was also confirmed by later molecular dynamics studies.[15] In turn, the associated singularity in the effective macroparticle's charge, due to an excess in the counterion's compensation of the bare surface charge, is known as charge reversal (CR), and the too simplified PB formalism cannot describe it since its occurrence involves strong ion-size correlations. Recently, direct measurements of CR were performed by Besteman *et al.*,[16–18] who employed atomic force microscopy

a)Electronic mail: marcelo@imp.mx.

techniques and a new electrophoresis capillarity apparatus to achieve laboratory conditions that were very difficult, or even impossible, to reach in traditional static and electrokinetic experiments. Posterior computer simulations for a size-symmetric electrolyte also showed the CR effect.[19–21] In these works the relevance of the ionic size, i.e., of the entropic contribution, for CR is proved. In particular, it has been shown[21,22] that depending on the ionic size, CR is possible even for a macroion in a monovalent electrolyte or may not be present in a divalent electrolyte, contrary to the general belief. Additionally, the oscillatory behavior of the ionic concentration profiles linked with CR and absent in the PB theory has been widely evidenced by different theoretical approaches[12,23–30] and by Monte Carlo (MC) simulations of planar,[31] cylindrical,[32] and spherical[33,34] EDLs.

Through the years, the experimental advances have prompted the development of theoretical explanations for CR. In this way, the theory of integral equations (IEs) for liquids has proven to be a robust and reliable approach in this area of research. For instance, it has been the main route to demonstrate that the ionic excluded volume constitutes, by itself, a physical mechanism with the ability to induce CR,[35,36] although this does not mean, naturally, that the CR observed experimentally under very diverse conditions is due purely to such steric effects (an interesting discussion about the physical and/or chemical origins of CR is available[37]).

Another fascinating phenomenon that has been theoretically predicted to occur in the EDL is overcharging (OC). OC appears when the coions are adsorbed to the electrified interface despite the Coulombic repulsion, *increasing* the native surface charge. This anomaly (the augmentation of the effective interface charge) was first observed and defined for a mixture of macroions and a size-symmetric electrolyte in contact with a charged wall[38] and should not be confused with CR (the reversion of the effective interface charge) since, unfortunately, in the literature CR has been frequently referred to as OC.[10,36,37,39] However, we insist that the only true OC is that reported in the 2004 paper.[38] In such article it was established that the OC was prompted by the macroions, whereas here we will show that OC can be present even in a simpler system (without a wall) if ionic size asymmetry comes into play. In this context, it is worth to recall that the most basic way to incorporate *consistently* ionic size contributions into the EDL is by using the so-called primitive model (PM) of an electrolyte, wherein the ions are taken as hard spheres, of arbitrary diameters, with point charges embedded at their centers. A large amount of work has been reported for the EDL using the PM in the special case of equal-sized ions [i.e., the restricted PM (RPM)], which implies a considerable simplification at the level of the model and calculations.[12,21,25,26,36,40–51] Notwithstanding, it is more realistic to expect EDL systems with different ionic sizes in their electrolytic species (due, for instance, to a distinct degree of hydration of the ions), and thus, the PM should be preferred for a more faithful representation of the EDL.

Along these lines, the issue of the practical relevance of ionic size asymmetry in the physical chemistry of surfaces has been recently revivified in an experimental paper on the electrokinetics of uncharged colloids by Dukhin *et al.*[52] In such investigation, the authors revisited the idea that "… a DL might in fact exist, even when there is no electric surface charge at all (on the colloid), solely because of the difference in cation and anion concentrations within the interfacial water layer …" and provided a measurement technique and experimental data supporting the existence of the so-called zero surface charge (ZSC) DL, a concept introduced in a theoretical model by Dukhin himself and co-workers more than 2 decades ago.[53–55] This result was corroborated in Ref. 38. The relevant fact to our discussion is that as proposed also by Dukhin and other authors,[56–62] such a difference in cation and anion concentrations and the concomitant charge separation in the proximity of an uncharged colloid can be attributed to the difference in the distances of closest approach of counterions and coions to the surface (as an alternative or in addition to the "chemical" phenomenon of specific adsorption). Thence, the work by Dukhin *et al.* emphasizes the importance of the ionic size asymmetry in relevant phenomena occurring in real EDL systems, such as the binding of simple inorganic electrolyte ions on colloidal substrates and electrokinetics.

It is interesting that in the literature there are relatively few publications considering ionic size asymmetry,[6,35,63–72] most of them dedicated to the planar geometry and only one extensive report for the spherical case.[6] In our opinion, this apparent lack of interest in size-asymmetric electrolytes might arise from the long-standing belief in the dominance of counterions in the EDL, a fact foreseen and corroborated in a couple of pioneering papers on the modified Gouy–Chapman (MGC) theory for planar interfaces.[63,64] To be more explicit, the precise meaning of the dominance of counterions is that "… at large potentials or charge densities, the coions are excluded from the vicinity of the electrode. Consequently, the counterions dominate and the DL properties approach those of a symmetric electrolyte whose charge and diameter are equal to those of the counterions …."[64] Noticeably, and even if this behavior was originally enunciated and verified *exclusively at the MGC level*, during the past years most of the modern studies of the EDL that use theoretical approaches that surpass the punctual-ions PB treatment have subscribed (or assumed without a rigorous proof) such counterion predominance in the PM,[30,31,47,66,67,69,73,74] a situation that has resulted in the mentioned scant attention to size-asymmetric EDLs. In contrast, recently, some of the present authors have published an IE and simulation analysis of the cylindrical[21] and spherical[6] EDL where it has been evidenced that for highly charged surfaces, counterions do not always dominate, i.e., that coions really matter in the DL. At this point, it should be also noted that the establishment of the counterion dominance by Valleau and Torrie[63] and Bhuiyan *et al.*[64] was not really based on the *plain* PB equation or equivalently on a model of a genuine punctual electrolyte since for these authors, the ion-ion potential corresponds to that between point charges, whereas for the ion-wall interaction a closest approach distance (hard-core or Stern correction) is added. In fact, the unequal-radius modified GC (URMGC) approach in Refs. 63, 64, and 75 represents not only the inclusion, at the lowest order, of excluded volume contributions into the GC theory

(via the Stern modification) but also the first attempt to take into account the ionic size asymmetry through the use of different distances of closest approach for counterions and coions. From all the above discussed, the new IEs results for a colloid in contact with a size-asymmetric PM electrolyte[6] (in which hard-core contributions are consistently embodied in both the ion-surface and ion-ion interactions) imply that an incomplete consideration of excluded volume and size asymmetry contributions, such as that of the URMGC theory, can lead to an inaccurate description of the DL at high surface charges.

Apart from the dominance of counterions at large electric fields, URMGC has predicted other notable phenomena in the EDL, this time for low-charged surfaces, such as the appearance of a potential of zero charge (PZC), oscillations in the ionic density and mean electrostatic potential (MEP) functions, and indeed CR and OC.[75,76] In the past years, several theoretical and simulation investigations[69,70,77] have pondered the planar EDL for a PM electrolyte in the low-charge regime and have corroborated the existence of the PZC and the nonmonotonic behavior of the ionic radial distribution functions (RDFs) and potential profiles, previously seen in the "semipunctual" URMGC. Nevertheless, in the same reports it was also found that only those theoretical formalisms [e.g., the MPB5 (Ref. 77) and density functional theories[70]] that fully include the hard-core and ionic size asymmetry effects succeeded in describing quantitatively the EDL near the point of zero charge,[70] contrasting with URMGC that showed solely a limited success for 1:1 salts.[69] In addition and with respect to CR and OC, in a 2006 paper[75] Yu *et al.* noticed, for the first time, the appearance of these "anomalies" in an URMGC treatment of an electrolyte inside a charged slit, a certainly intriguing fact given that, in the past, CR and OC had been observed only in theoretical analysis of PM EDLs.[36,38] Therefore, at present, an exhaustive simulation study that confirms and characterizes the phenomena of CR and OC in *slightly* charged PM EDLs, as well as an application of reliable theories in order to explain these striking features, is still lacking in the literature. Precisely, the main objectives of this communication are, in the first place, to supply fresh and comprehensive MC data about the PZC, CR, OC, and the behavior of diverse structural properties of a low-charged PM EDL in spherical geometry and, second, to present the comparison of such simulation information with the corresponding theoretical results of the HNC/MSA and URMGC IEs, trying to assess the consequences of a consistent treatment of the excluded volume and ionic size asymmetry contributions in the SEDL.

To investigate the static properties of the size-asymmetric SEDL in the weakly charged regime, with special focus on the CR and OC phenomena, we have produced simulation and HNC/MSA IE results for the RDFs of 1:1 and 2:2 PM electrolytes bathing a spherical colloid under diverse conditions. From the RDFs we extract the MEP and the charge profiles to identify the presence of CR and OC and to examine their dependence on the ionic size asymmetry and other system parameters. All this structural information is contrasted with that corresponding to the semipunctual URMGC theory. As it will be illustrated below, most of the computer "experiments" data are better paralleled by HNC/MSA than by URMGC. We would like to note that to the best of our knowledge, this work reports the first confirmation, via simulations, of CR and OC in the PM EDL near the point of zero charge. Additionally, we present a fundamental statistical mechanics explanation of the OC and CR effects reported here. This paper is organized as follows. In Sec. II we present the model system and the theoretical approaches. Section III contains the details of the numerical solution of the IEs and of the MC simulations. Section IV is devoted to the results and their discussion, and we close with a summary of relevant findings and conclusions in Sec. V.

II. MODEL SYSTEM AND THEORY

Our basic representation of the spherical EDL (SEDL) is constituted by a rigid charged spherical colloid of diameter D_0 and uniform surface charge density σ_0 surrounded by a continuum solvent of dielectric constant ϵ. The macroion is in contact with two ionic species, which in the PM are treated as hard spheres of diameters D_i $(i=1,2)$ with embedded point charges, q_i, at their centers. Note that $q_1 q_2 < 0$. The interaction potential between the particles in this model (i.e., macroion and electrolytic ions) is then given by

$$U_{ij}(r) = \begin{cases} \infty & \text{for } r < D_{ij} \\ q_i q_j/(\epsilon r) & \text{for } r \geq D_{ij}, \end{cases} \tag{1}$$

where the subscripts i and j run from 0 to 2, r is the center-to-center distance between two particles of types i and j, $D_{ij}=(D_i+D_j)/2$, $q_i=z_i e$ is the charge of the species i with valence z_i, e is the protonic charge, and, for the spherical colloid, $q_0=z_0 e=4\pi(D_0/2)^2\sigma_0$. The system as a whole is electroneutral, i.e., $\Sigma_{j=1}^{2} z_j \rho_j = 0$, where ρ_j is the bulk number density of the electrolytic species j.

The Ornstein–Zernike equation for a homogeneous multicomponent mixture of S species (with spherical symmetry) is[78]

$$h_{ij}(r) = c_{ij}(r) + \sum_{k=0}^{S-1} \rho_k \int h_{ik}(t) c_{kj}(|\vec{r}-\vec{t}|) d^3 t, \tag{2}$$

such as ρ_i is the bulk number density of each one of the species in the system, $r=|\vec{r}|$ and $h_{ij}(r)$ are respectively the distance and the total correlation function between two particles of types i and j, $g_{ij}(r)=h_{ij}(r)+1$ is the RDF, $c_{ij}(r)$ is the direct correlation function, and $t=|\vec{t}|$ is the distance between two particles of types i and k. This group of equations requires a second relation (or closure) between the total and direct correlation functions. For charged systems, the hypernetted chain (HNC) and the mean spherical approximation (MSA) closures are widely used.[78,79] The HNC and MSA relations, for $r \geq D_{lm}$, are given as

$$c_{lm}(r) = -\beta U_{lm}(r) + h_{lm}(r) - \ln[h_{lm}(r)+1] \tag{3}$$

for HNC and

$$c_{lm}(r) = -\beta U_{lm}(r) \tag{4}$$

for MSA, where $\beta=1/(k_BT)$ is the inverse of the thermal energy. These expressions are complemented by the exact condition $h_{lm}(r)=-1$, for $r<D_{lm}$.

Let us consider $S=3$ and that the species 0 corresponds to macroions (thereinafter denoted equivalently by M) at infinite dilution, whereas the indices 1 and 2 are associated to a binary electrolyte. Then Eq. (2) for the components $M(\equiv 0)$ and j can be written as

$$h_{Mj}(r) = c_{Mj}(r) + \sum_{k=1}^{2} \rho_k \int h_{Mk}(t) c_{kj}(|\vec{r}-\vec{t}|) d^3t, \quad j=1,2. \tag{5}$$

Note that Eq. (5) is a complete set of IEs for the SEDL. When Eq. (3) is employed in Eq. (5) solely for $c_{Mj}(r)$ and the $c_{kj}(|\vec{r}-\vec{t}|)$ are approximated by the MSA analytical expressions for a bulk electrolyte,[80–82] the HNC/MSA IEs are obtained. A detailed account of this HNC/MSA formalism can be consulted elsewhere[6] and will not be repeated here. Our election of the HNC/MSA theory to perform the present study is based on the fact that for many years, it has been used successfully to investigate the RPM EDL in many geometries (e.g., planar, cylindrical, and spherical).[6,12,25,26,33,34]

The integral version of the URMGC theory in *spherical geometry* is easily deduced from the HNC/MSA formulation if $c_{kj}(|\vec{r}-\vec{t}|)=-\beta q_k q_j/(\epsilon|\vec{r}-\vec{t}|)$ is inserted in Eq. (5) instead of the interionic MSA direct correlation functions. It must be stressed that in the original papers,[63,64] as well as in all the posterior treatments,[69,75] URMGC has been solved, in differential form, strictly for planar interfaces, which means that the present study extends the classic URMGC planar theory to the spherical instance, continuing along the lines of our previous URMGC (and HNC/MSA) account of the SEDL.[6]

Once the $g_{Mj}(r)$ are available, either from a theory (e.g., HNC/MSA or URMGC) or from simulation, it is then possible to calculate various relevant functions, namely, the total integrated charge (IC),

$$P(r) = z_M + \int_0^r \sum_{j=1}^{2} z_j \rho_j g_{Mj}(t) 4\pi t^2 dt, \tag{6}$$

and the MEP,

$$\psi(r) = \frac{e}{\epsilon} \int_r^\infty \frac{P(t)}{t^2} dt. \tag{7}$$

These quantities are fundamental in our analysis of the properties of the SEDL. The IC is a measure of the net charge (in units of e) enclosed in a sphere of radius r centered in the macroion. It equals z_M for $D_0/2 \le r \le (D_0+D_1)/2$ if $D_1<D_2$ and goes to zero as $r\to\infty$ due to the electroneutrality condition. The IC also allows to compute the amount of charge adsorbed onto the macroparticle, i.e., the accumulated charge within the Helmholtz planes (see below for the definition of the Helmholtz planes), and, moreover, it detects CR when $P(r)z_M<0$ and OC if $P(r)z_M>0$ and $|P(r)|>|z_M|$. In addition, the MEP around the macroion is a central magnitude in colloid science because it determines, for instance, the regimes of stability/flocculation or the migration of macroparticles in a colloidal suspension.[83] As a matter of fact, the MEP at certain distance near the macroion's surface is usually identified with the well-known electrokinetic potential at the slipping plane (or zeta potential, ζ).[3,83] The ζ potential is experimentally measurable in systems that display electrokinetic effects such as electrophoresis, electroosmosis, and streaming currents, and it has an ample use in the physicochemical characterization, separation, and/or fabrication of colloidal materials.[2,84]

In particular, we will be interested in the IC and the MEP in the neighborhood of the Stern layer. More specifically, the Stern layer is the free-of-ions space next to a macroion that ends at the Helmholtz plane. The Helmholtz plane (or, more properly, the Helmholtz surface) is the geometrical place associated to the colloid-ion closest approach distance.[3,83] In size-symmetric electrolytes only one Helmholtz plane can be identified. In our model, however, the size asymmetry between the ions allows us to define an inner Helmholtz "plane" (IHP) and an outer Helmholtz plane (OHP) (note the conventional usage of the word plane). The IHP is specified by the closest approach distance of the smallest ionic component to the colloidal surface [i.e., by $(D_0+D_1)/2$ if $D_1<D_2$], whereas the OHP is determined by the corresponding distance of closest approach for the largest species [i.e., by $(D_0+D_2)/2$ if $D_1<D_2$]. Therefore, for the PM EDL if $D_1<D_2$, the Stern layer is the region where $D_0/2 \le r < (D_0+D_1)/2$, and the Helmholtz zone corresponds to $(D_0+D_1)/2 \le r \le (D_0+D_2)/2$. Obviously, for size-symmetric salts the IHP and the OHP coincide, and the standard notions of the Helmholtz plane and Stern layer are recovered. In the general PM case and provided that $D_1<D_2$, when the MEP is evaluated at $r=(D_0+D_1)/2$, Eq. (7) gives the MEP at the IHP, which we denote as ψ_{IHP}. On the other hand, if Eq. (7) is calculated at $r=(D_0+D_2)/2$, the MEP at the OHP, ψ_{OHP}, is obtained.

Equation (5) for HNC/MSA can be recast as[38,85,86]

$$W_{Mj}(r) = -k_BT\, ln[g_{Mj}(r)] = z_j e\psi(r) + J_{Mj}(r), \tag{8}$$

such as $W_{Mj}(r)$ is the potential of mean force between the macroparticle and an ion of species j, separated by the distance r. Thus, $W_{Mj}(r)$ is the necessary energy to bring the ion from infinity to the distance r from the macroparticle. $V_j(r)\equiv z_j e\psi(r)$ is the corresponding electrostatic energy, and $J_{Mj}(r)$ is a fluctuation term related with the ionic sizes, i.e., an energy associated to the system's excluded volume, hereinafter referred to as an entropic contribution. Notice that for the PB theory, $J_{Mj}(r)=0$. *Although, in Eq. (8) the electrostatic and hard spheres terms are apparently independent, they are correlated since to obtain $\psi(r)$ and $J_{Mj}(r)$ we need to express them in terms of $g_{Mj}(r)$ and solve the non-linear HNC/MSA IE. Therefore the energetic and entropic contributions to the structure of the SEDL are not really separable.*

III. NUMERICAL DETAILS

A size-asymmetric 1:1 or 2:2 electrolyte with a ratio between ionic diameters $D_-/D_+=2$, bathing a charged macroparticle of diameter $D_M=D_0=20$ Å and valence z_M, was considered in all the calculations reported. Specifically, the diameters of the positive and negative species were $D_+=4.25$ Å and $D_-=8.5$ Å, respectively. In other words, for definitiveness, the cations have been chosen as the smallest species of the binary electrolyte, i.e., $D_+=D_1$ and $D_-=D_2$, with $D_1<D_2$. Note also that the sign of z_M defines which one of the ionic species is the coion or counterion.

We should point out that for a macroparticle diameter of 160 Å, either of cylindrical[12] or spherical[26] geometry, the EDL practically becomes that of a plate (i.e., where the radius is infinite), and we would lose the relevance of the spherical geometry. While spherical proteins, dendrimers, micelles, and other colloids can have a diameter as small as 10 Å,[1–3,84,87–89] this diameter is perhaps too small[12,26] for many systems. Hence, we have chosen $D_M=20$ Å as a compromise between the macroparticle diameter and the larger negative ions size ($D_-=8.5$ Å). A diameter for a negative hydrated ion of $D_-=8.5$ Å is in the range of some real systems of interest, for example, the hydrated nitrate anion has an approximate diameter of 6.8 Å, whereas that of the hydrated phosphotungstate anion is 9.4 Å.[90–92] Finally, this ionic size has been used in the past, in theoretical planar EDL studies.[35]

To establish the primitive and semipunctual models employed in our simulation and theoretical approaches, let us introduce the macroion-ion contact distances, d_{M+} and d_{M-}, given by

$$d_{Ml}=\begin{cases}(D_M+D_+)/2 & \text{for } l=+\\ (D_M+D_-)/2 & \text{for } l=-.\end{cases} \tag{9}$$

It must be remembered that here the macroions, cations, and anions correspond to the indices 0 (or M), 1, and 2, respectively.

Complementarily, the ion-ion contact distances, d_{++}, d_{--}, and $d_{+-}(=d_{-+})$ are

$$d_{ij}=\begin{cases}D_+ & \text{for } i=j=+, \text{ in simulation and HNC/MSA,}\\ D_- & \text{for } i=j=-, \text{ in simulation and HNC/MSA}\\ (D_++D_-)/2 & \text{for } i=+ \text{ and } j=-, \text{ in simulation and HNC/MSA}\\ 0 & \text{for any } i \text{ and } j, \text{ in URMGC.}\end{cases} \tag{10}$$

The dielectric constant and temperature considered in all the cases were $\epsilon=78.5$ and $T=298$ K.

The URMGC and HNC/MSA theories were numerically solved by means of a Picard iteration scheme, which, in the past, has been thrivingly employed in a number of studies of the EDL in various geometries via IEs and density functional theories.[6,47,51]

Simulations were performed in a cubic box with the usual periodic boundary conditions in the canonical ensemble. The ionic species satisfied the electroneutrality condition: $z_M+N_+z_++N_-z_-+N_cz_c=0$, where z_M is the valence of the macroion, N_+, z_+ and N_-, z_- are the number of ions and the valence of the positive and negative species in the added salt, respectively, and N_c and z_c are the number and the valence of the counterions that balance the colloidal charge. In order to accomplish consistent comparisons with the theory, the absolute value of the valence of such counterions was $|z_c|=1$ for the 1:1 electrolyte and $|z_c|=2$ for the 2:2 salt. The macroion was fixed in the center of a simulation box of length L, and in order to avoid border effects, the extension of the cell was enlarged until the IC showed clearly a plateau of zero charge far from the macroion. The runs were done for $\approx$2000 particles for the monovalent salt and $\approx$1000 ions for the divalent electrolyte. The long-range interactions were taken into account by using the Ewald sum technique with conducting boundary conditions.[93,94] The associated damping parameter was $\alpha=5/L$, and the $\vec{k}$-vectors employed to compute the reciprocal space contribution satisfied the condition $|\vec{k}|\leq 5$. MC runs of charged systems were performed with 5×10^4 equilibration MC cycles and from 6×10^5 to 1.8×10^6 MC cycles were practiced to obtain the canonical average. The RDFs were calculated using standard bin procedures,[93,94] whereas the IC and the electrostatic potential were obtained by using Eqs. (6) and (7), respectively.

IV. RESULTS AND DISCUSSION

In what follows our results are discussed chiefly in terms of the MC simulations data. Appropriate comparisons with the HNC/MSA and URMGC formalisms are presented such that the accuracy of the theoretical predictions can be assessed.

A. Monovalent size-asymmetric electrolytes

The structure of the EDL is the result of an entropic and energetic competition. In the proximities of the point of zero charge the entropy is expected to be important, whereas for highly charged macroparticles the EDL should exhibit strong Coulombic correlations. Thus, in order to understand the behavior of the ionic atmosphere next to a barely charged colloid in contact with a size-asymmetric electrolyte, we will first present a comparison between the surrounding distribution of a univalent salt and that of a mixture of hard spheres (with the same radii and concentration). This will illustrate how the structure of charged systems deviates from the neutral situation.

Let us consider initially the ionic distribution around an uncharged macrosphere ($z_M=0$). Figure 1 displays the MC, HNC/MSA, and URMGC RDFs of two systems; in one case the ionic species represent a 1:1 1M salt, and in the other the "ions" are uncharged, forming a pure hard-sphere assembly. We note here that in the former system, the EDL is the result of both the entropic and energetic contributions; in contrast, the structure of the latter instance is only driven by entropy because all the interactions are of the excluded volume type. Nevertheless, since we are working in the zero colloidal

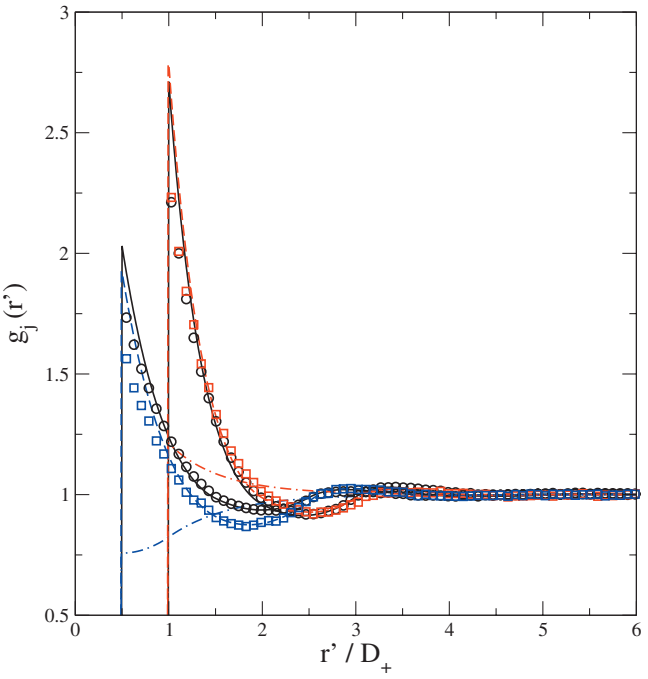

FIG. 1. RDFs of a size-asymmetric binary mixture of hard spheres and a size-asymmetric 1:1 electrolyte, both at a 1*M* concentration, around an uncharged (z_M=0) macroparticle as a function of the distance to the surface of the colloid. Thereinafter, the diameters of the ionic species and colloid are D_+=4.25 Å, D_-=8.5 Å, and D_M=20 Å, respectively. The small hard spheres have the same diameter as that of the cations, $D_1=D_+$, and the large hard spheres' diameter is the same as that of the anions, $D_2=D_-$. Hence, the distance of closest approach of the small hard spheres and cations is at $r'/D_+=0.5$, and the distance of closest approach of the large hard spheres and anions is at $r'/D_+=1$. The open circles correspond to MC simulations of the size-asymmetric mixture of hard spheres, and the open squares represent the MC data of the size-asymmetric monovalent electrolyte. The solid lines are associated to the asymmetric mixture of hard spheres in the HNC/MSA approach. The dashed and dot-dashed lines are the HNC/MSA and URMGC results for the 1:1 size-asymmetric salt, respectively.

charge regime, we expect that in the first case the excluded volume interactions play a determinant role in the resulting properties of the DL. This is corroborated in Fig. 1, as it is explained in the following. An inspection of the MC data of the charged and uncharged systems shows that the structure of the two cases is rather similar for $r'/D_+>2.5$ (where r' is the distance measured from the colloidal surface), indicating the existence of weak charge correlations at these distances. Differences, however, are noticeable at smaller distances, particularly for the tiniest species. We observe that the addition of charge to the ionic species slightly increases the concentration of the larger species and decreases the concentration of the smaller species, especially at the contact distances. As it is shown later, this dewetting of the surface, by the small ions, augments with the valence of the ions as a result of the larger electrostatic self-interaction energy of the system. Notice that being the concentration and charge of the positive and negative ions the same, the larger negative ions have a larger contact concentration near the macroparticle due to a higher entropic contribution associated with their size. In other words, the larger the size of the ions, the larger their adsorption to the macroparticle in order to increase the accessible volume (and the entropy). Such comportment of the RDFs could lead eventually to significant changes in the thermophysical properties of the charged systems since, for instance, the pressure depends directly on the contact values of the pair correlation functions.[78,79] We must point out that these are rather concentrated systems, with an ionic volume fraction of $\phi\approx0.217$. That is the reason why the contact peaks of the neutral system are so high. Hence, at these volume fractions, the charge correlations in the neighborhood of the macroparticle are masked by the strong steric contributions. Notwithstanding, we remark that for barely charged systems, the absolute values of the ionic RDFs close to the surface and the extent of their deviations with respect to the pure hard-sphere mixture will rule the behavior of the IC and MEP and will be crucial to the degree of appearance of CR and OC, as it is evidenced below.

As such, an adequate theoretical description of the present EDL systems will depend on its ability to capture correctly the electrostatic and steric correlations close to the macroparticle. In this regard, the IEs results portrayed in Fig. 1 illustrate that HNC/MSA follows closely the trends of the simulations, with quantitative discrepancies near the colloid where this scheme overestimates the RDFs. In contrast, the URMCG data exhibit very different tendencies from those of the simulations. Especially noticeable is the pronounced separation between the URMGC RDF of small ions and those from HNC/MSA and MC, as well as the very low values of the same URMGC normalized density of cations in the zone comprised by the Helmholtz planes. In fact, such exaggerated absence of small ions in URMGC is a sequel of the neglect of the ionic size in the ion-ion interactions, which denotes the importance of the entropic contribution to the EDL and will be of consequence in our later analysis of CR and OC. Also, and contrary to the MC data, the URMCG theory predicts $g(r)$'s that are monotonic beyond the OHP, a well documented characteristic of point-ions theories.[2,3,83] From all the previous discussion, it is therefore expected that the ensuing properties of the EDL extracted from the HNC/MSA and URMGC ionic profiles should present important discrepancies between them, with HNC/MSA excelling in the comparison with MC.

In Fig. 2 the corresponding IC is graphed as a function of the distance to the surface of the macroion. Interestingly, we note that all the simulation and theoretical IC curves present the adsorption of a layer of positive charge (small ions) very close to the macroion's surface; such layer begins at the IHP and reaches its maximum value of charge at the OHP since it is at the OHP where the large ions begin to contribute with their negative charge. The maximum indicates that the positive (little) ions overcompensate the negative (large) ions charge. The amount of charge in the Helmholtz zone is significant ($\approx3.8e$, $4.1e$, and $2.2e$ for MC, HNC/MSA, and URMGC, respectively) and, in turn, gives rise to the formation of a DL beyond the OHP (see Fig. 1). The existence of this ZSC-DL in our calculations is rewarding since it confirms the ideas originally proposed by Dukhin *et al.*[52–55] and, in addition, agrees with other studies of the ZSC-DL in planar geometry via MC simulations,[69] IE theories,[38] the URMGC,[63,64,75] and density functional theories.[70] In our MC and HNC/MSA cases, after its maximum, the IC decreases until changing sign and,

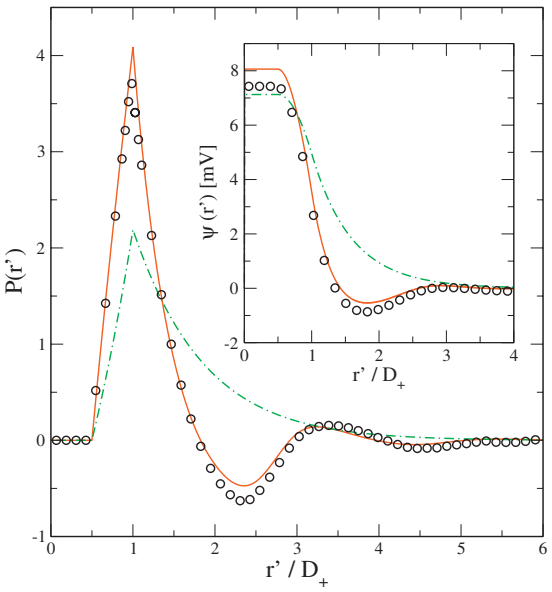

FIG. 2. IC (main panel) and MEP (inset) of a size-asymmetric 1:1 1*M* electrolyte around an uncharged ($z_M=0$) macroparticle as a function of the distance to the surface of the colloid. The open circles, solid, and dot-dashed lines correspond to the MC, HNC/MSA, and URMGC data, respectively.

subsequently, exhibits a region of negative values for $1.8 \lesssim r'/D_+ \lesssim 3.0$. Farther than $r'/D_+=3.0$ the accumulated charge fluctuates around zero, and finally, the electroneutrality condition is obtained when $r' \to \infty$. Contrarily, the $P(r')$ of URMGC goes uniformly to zero.

The information presented so far evince that at the point of zero charge, a very simple 1:1 salt in contact with a macroparticle already displays highly nonlinear effects such as charge adsorption (i.e., a ZSC-DL) or the reversion in the sign of the IC. These phenomena are due to both the finite ionic size and to the asymmetry between the electrolytic species of the model. Since HNC/MSA fully incorporates such conditions, it is able to reproduce all the characteristics observed in the simulations even at a quantitative level. In contrast, URMGC does not embody completely the ionic size correlations, just the nonzero contact distances between the colloid and ions. This is just enough to capture the adsorption of charge but not the additional traits of the accumulated charge at intermediate and large r'. In particular, URMGC fails to detect the sign reversal in $P(r')$, predicting instead a monotonic neutralization of the effective charge adsorbed inside the Helmholtz planes. In other words, the partial inclusion of the ionic size and size asymmetry contributions in URMGC has the severe inconvenience that in this semipunctual approach, the occurrence of some of the steric-related peculiarities, such as the ZSC-DL, CR, and the oscillation of the RDFs and IC, is restricted exclusively to the region between the Helmholtz planes. This fact, to which we will refer to as *the localization of the ionic size and size asymmetry effects in URMGC*, will be a recurrent issue in our posterior discussions of the structural properties, CR and OC.

The MEP as a function of the distance to the uncharged macroparticle is plotted in the inset of Fig. 2. The first thing worth to be noticed is that despite a zero charge on the colloid, the MC, HNC/MSA, and URMGC MEPs at the IHP are positive. This PZC has been largely recognized as a direct consequence of the ionic size asymmetry in the EDL since the initial papers by Valleau and others,[63,64] and in the mean time, it has received great attention in diverse simulation and theoretical accounts of the planar DL.[35,69,70] Evidently, this PZC is due to the dominant population of cations close to the macroion, which in turn is originated by the different entropy-driven adsorption, associated to the unequal ionic sizes. Far from the surface of the macroion, the MEPs of MC and of HNC/MSA tend to zero, but for intermediate distances they have a series of minima and maxima of alternating sign. In particular, the first minimum defines the region where the MEP reversal is stronger. Now, if the wanted association between the electrokinetic and MEPs is invoked,[3] the graphed comportment of the MEP suggests that *a macroparticle could experience electrophoresis even if it is uncharged*. Thence, for small cations and depending on the precise localization of the slipping surface,[83] the neutral colloid should move in the direction of the applied field if this surface is somewhere in between the Helmholtz planes or backward if the shear boundary is situated around the position of the first MEP minimum. It is generally accepted that the slipping or ζ-plane is very close to the surface of the macroions;[83] therefore we expect the first scenario to be more plausible. Note that for small cations, UMRGC foresees that the macroparticles should flow always in the direction of the external electric field.

So far we have examined systems at the point of zero charge, i.e., with a noncharged central macroion. In spite of that, the colloid-ion entropic contributions and the interionic correlations led to interesting phenomena, i.e., macroparticle-ions electrical correlations appear. Although the central colloid is uncharged, the adsorbed little ions effectively charge it. Now, by weakly charging the macroions, conspicuous effects such as CR and OC arise, as it is seen in the remaining of this section. Then, let us evaluate two situations in which the valence of the macroion is $z_M=-4$ and $z_M=4$ (i.e., surface charge densities $\sigma_0=\pm 0.051$ C/m^2), with the same 1:1 electrolyte as before. Note that by virtue of z_M, the role of anions and cations as counterions or coions is interchanged. Figure 3 includes the RDFs of the electrolyte around the macroion for the two values of z_M. Figure 3(a) contains the case in which the counterions are smaller than the coions ($z_M=-4$), whereas the case of larger counterions ($z_M=4$) is reported in Fig. 3(b). Figure 3(a) reveals that compared to the RDFs of a neutral macroparticle in Fig. 1, the presence of the counterions in MC and HNC/MSA is greater when the surface is negatively charged, as evidenced by the increased contact peak, whereas the concentration of coions diminishes. This fact stresses the relevance of charge correlations (induced by z_M) on the ordering of the ions around the macroparticle. The RDFs of URMGC visibly disagree with MC and HNC/MSA. On the other hand, for $z_M=4$ [now the counterions are larger than coions; Fig. 3(b)], we see a dramatic decrement in the contact peak of the smaller ions (coions) and an augment in that of the larger ions (counterions), which are adequately reproduced by HNC/MSA and

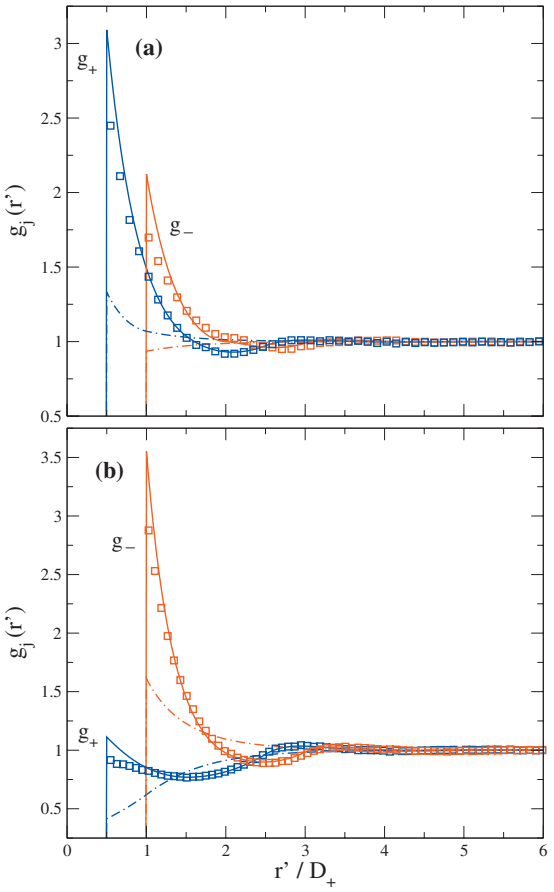

FIG. 3. RDFs of a size-asymmetric 1:1 1*M* electrolyte around a charged macroion as a function of the distance to the surface of the colloid. In (a) $z_M=-4$, and in (b) $z_M=4$. The open squares, solid, and dot-dashed lines represent the MC, HNC/MSA, and URMGC results, respectively.

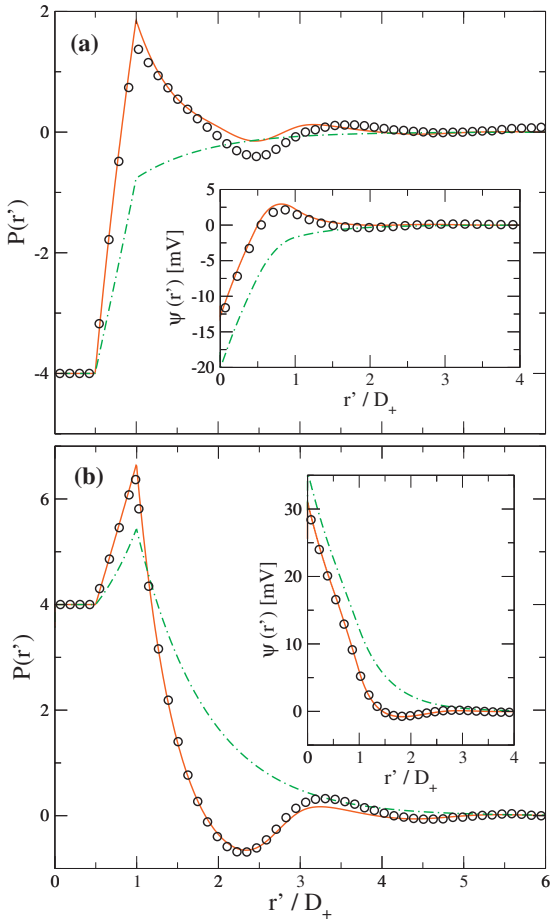

FIG. 4. IC (main panels) and MEP (insets) of a size-asymmetric 1:1 1*M* electrolyte around a charged macroion as a function of the distance to the surface of the colloid. In (a) $z_M=-4$, and in (b) $z_M=4$. The open circles, solid, and dot-dashed lines correspond to the MC, HNC/MSA, and URMGC data, respectively.

not by URMGC. Since we are dealing with charged systems, size and charge correlations are not independent of each other.

Further details can be grasped by looking at the $P(r')$ curves, as they are presented in Fig. 4. For $z_M=-4$ [Fig. 4(a)] we find that the MC IC increases almost linearly inside the Helmholtz planes, inverting its original sign (*i.e., experiencing CR*) and reaching a maximum of $P_{\max}(r')\approx 1.3$ at the OHP. After the OHP, $P(r')$ acquires a fluctuating behavior, where subsequent charge inversions can be appreciated. In the past it was believed that CR could occur only for divalent salts. Later,[21,36,38] it was shown that monovalent salt could show CR if the ionic size or concentration is sufficiently large or in the presence of a third uncharged species since, in this last case, the additional component increases the excluded volume and then augments the ionic adsorption to the macroparticle in order to compensate the accessible volume. Here, we demonstrate that monovalent salts can present CR also when there is an ionic size asymmetry. In addition, we will evidence that the 1:1 CR is, in fact, larger than that for the 2:2 case. These features are perhaps not well recognized in the literature of CR. The inset of Fig. 4(a) indicates that the MEP of MC is also oscillatory, with a maximum inversion inside the Helmholtz zone. The level of accuracy of the analyzed theories can be readily estimated from the main panel and its inset. Particularly, we see that differently from HNC/MSA, URMGC is unable to describe any reversal of the accumulated charge or the MEP throughout all the space. This represents an extreme manifestation of the so-called localization of the ionic size and size asymmetry effects in URMGC.

The functions $P(r')$ and $\psi(r')$ for $z_M=4$ are portrayed in Fig. 4(b) and its inset. Notably, the MC $P(r')$ *increases* in between the Helmholtz planes, revealing *an adsorption of charge of the same sign as that of the macroion*, which in turn "augments" the native macroion charge up to a maximum value of $P_{\max}(r')\approx 6.3$ at the OHP. This striking event is referred to as *OC*. OC was predicted theoretically by Jiménez-Ángeles and Lozada-Cassou[38] for a charged wall in contact with a mixture of macroions and a fully-symmetric salt. *To this date, this peculiarity had not been confirmed in the PM EDL through simulations or experiments.* Hence, our results provide the first simulation evidence of OC in a very simple model, where such "anomaly" is a direct consequence of the ionic size asymmetry when charge correlations are not too strong, i.e., close to the point of zero charge. *In this sense, OC appears when size correlations dominate over charge correlations near the point of zero charge.* This implies, therefore, that OC is also expected in other geometries whenever ionic size asymmetry is present. We would like to

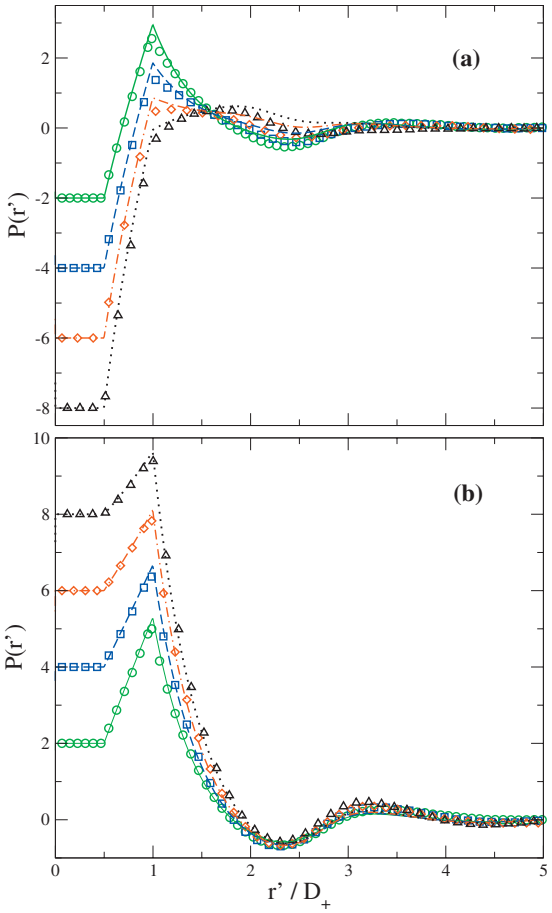

FIG. 5. IC of a size-asymmetric 1:1 1*M* electrolyte around a charged macroion as a function of the distance to the surface of the colloid. In (a) the open circles, squares, diamonds, and triangles correspond to MC simulations for $z_M=-2,-4,-6,-8$, respectively, and in (b) are associated to $z_M=2,4,6,8$, respectively. In (a) the solid, dashed, dot-dashed, and dotted lines correspond to HNC/MSA results for $z_M=-2,-4,-6,-8$, respectively, and in (b) are associated to $z_M=2,4,6,8$, respectively.

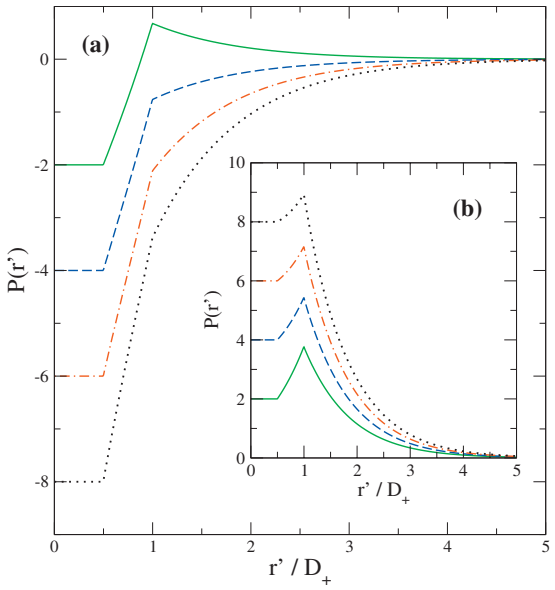

FIG. 6. The same as in Fig. 5 but for the URMGC theory. In the main figure the solid, dashed, dot-dashed, and dotted lines correspond to $z_M=-2,-4,-6,-8$, respectively, and in the inset to $z_M=2,4,6,8$, respectively.

point out that the OC results presented here are in line with our previous report,[6] where it has been established that the properties of the electric DL depend on the two species of a binary electrolyte, and not only on the counterions as it has been widely accepted. On the other hand, regarding the performance of the theoretical schemes we are working with, we realize that URMGC is capable to describe the OC but not the CR nor the oscillations observed in the MC data of $P(r')$ nor the inversion of the corresponding MEP. This fact is a typical expression of the URMGC restraint of all the excluded volume and size asymmetry phenomena to occur exclusively in the Helmholtz zone. Contrastingly, HNC/MSA collates very well with the simulation data, describing correctly all these characteristics.

To analyze the behavior of the IC as we depart from the point of zero charge, in Fig. 5 we present $P(r')$ of MC and HNC/MSA for negative and positive values of z_M. When counterions are smaller than coions [$z_M<0$; Fig. 5(a)], the maximum simulation CR observed at the OHP decreases as the valence of the macroion becomes more negative, as one could expect since the available room for adsorbed counterions to the macroion is finite. In fact, CR within the Helmholtz planes disappear altogether for $z_M\approx-7$. For $z_M<-7$ the first layer of CR shifts further away from the macroparticle. On the other hand, in the MC curves corresponding to coions smaller than counterions [$z_M>0$; Fig. 5(b)] OC occurs, and the difference between the peak of OC (at the OHP) and z_M (at the surface) decreases as z_M increases, which is the result of the growing macroion-coions repulsion. OC virtually disappears everywhere when this electrostatic repulsion becomes strong enough, which for this system corresponds to $z_M\approx24$ ($\sigma_0\approx0.3$ C/m^2). Consequently, the maximum of OC in the PM EDL only happens at the OHP, indicating that it is a feature directly caused by the size asymmetry of the ions in a PM binary electrolyte. The observed OC effect can be further enhanced depending on several factors, namely, ionic size asymmetry ratio, ionic charge and concentration, and macroion charge and geometry. Thus, our data remark the relevance of the coions in surface phenomena beyond the point of zero charge. From Fig. 5 the good coincidence between the simulations and the HNC/MSA theory is manifest.

The IC of URMGC does not follow any of the aforesaid tendencies. In the first place, for $z_M<0$ [Fig. 6(a)], such theoretical approach exhibits CR only for a colloidal charge of $z_M=-2$ and this reversal is weak [$P_{\max}(r')\approx0.7$ at the OHP], which means that differently from MC and HNC/MSA, the CR disappears already for $z_M<-2$. The origin of this comportment of the CR can be traced back to the very low values of the URMGC concentration of small cations near a discharged surface reported in Fig. 1. When the negative charge on the initially neutral colloid starts to grow (i.e., z_M becomes more negative), the small (and positive) counterions are attracted to the macroparticle and increase their number in the Helmholtz zone, then producing CR for very low z_M ($-2\lesssim z_M<0$, for URMGC). However, due precisely to the mentioned URMGC scarcity of small counterions at $z_M=0$, the growth of the negative surface charge overtakes that of the CR owed to the counterions, and rapidly sup-

presses it. Second, and in further contrast with MC and HNC/MSA, in the data in Fig. 6(a) we notice that once the reversal of charge in URMGC ceases to occur in the Helmholtz region (for $z_M \lesssim -2$), it is never observed again at any point beyond the OHP in the monotonically decreasing profiles of $P(r')$. Evidently, this is another example of the localization of the ionic size and size asymmetry effects in the semipunctual URMGC formalism. Complementarily, for $z_M > 0$ [Fig. 6(b)], the URMGC IC presents OC within the Helmholtz planes, which diminishes slowly as z_M augments. Notwithstanding, the OC in this theory is less important than that in simulations and HNC/MSA, as can be verified from a comparison of the respective differences $|P(r')-z_M|$. Besides, and as expected, the IC curves in Fig. 6(b) go uniformly to zero after the OHP. Such abatement of the OC in URMGC for positive surface charges can also be explained in terms of the low presence of small ions close to a discharged macroparticle. In this case, when the positive colloidal charge is being incremented from the zero value, the shortage of small cations (coions) available to build-up the OC in the proximities of the surface lessens the magnitude of the anomalous effect.

On the other hand, apart from the usual monotonicity of the URMGC IC as a function of the distance, in the two sequences of curves for different z_M presented in Fig. 6, we observe an extra monotonic character of the $P(r')$ profiles, this time with respect to the variation in z_M [or, equivalently, with respect to the change in $\sigma_0 = z_M e/(\pi D_M^2)$]. Specifically, in Figs. 6(a) and 6(b) the IC curves associated to distinct values of z_M (or σ_0) never cross each other. Thus, we find that in terms of the colloidal surface charge σ_0, the URMGC IC functions, for any fixed r', satisfy the condition

$$\frac{\partial P(\sigma_0, r')}{\partial \sigma_0} > 0. \tag{11}$$

Otherwise, and as can be noted in Fig. 5(a), the ICs of MC and HNC/MSA show regions where the alternative condition

$$\frac{\partial P(\sigma_0, r')}{\partial \sigma_0} < 0 \tag{12}$$

is satisfied. We realize that this last "anomalous" behavior is possible due to the presence of crossing points in the corresponding $P(r')$ profiles for distinct z_M [see Fig. 5(a)]. Physically, Eq. (11) establishes that if the charge over the macroion is increased, the corresponding effect in the SEDL is to augment locally the IC, which is intuitively awaited. Contrastingly, Eq. (12) states that the increase in the macroion's charge promotes a local decrease in the IC due to the excess of adsorbed ions in between the Helmholtz planes and to the ionic size correlations. We refer to this behavior as a *local inversion of the derivative of the IC*. It should be noted that such inversion of the derivative occurs only when $z_M < 0$. This same phenomenon seems to be absent for MC and HNC/MSA if $z_M > 0$ [see Fig. 5(b)] and, instead, it is apparent that all the IC profiles meet at their first minimum ($r'/D_+ \approx 2.3$). However, this inversion effect is indeed present also for $z_M > 0$ in the 2:2 electrolyte calculation, as it will be shown later. In the URMGC case there is CR and OC

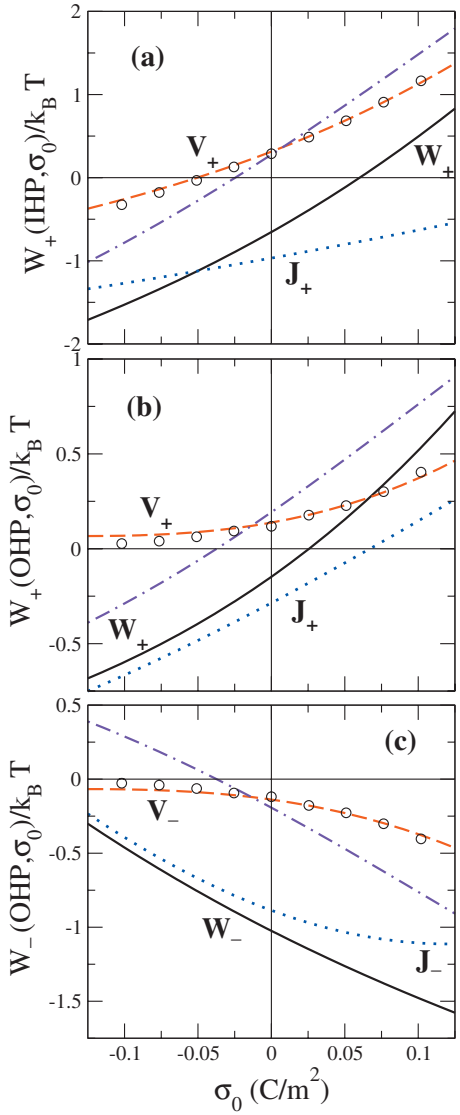

FIG. 7. Potential of mean force, W_j, of an ion of species j at the IHP and OHP as a function of the macroparticle surface charge density, σ_0, for a size-asymmetric 1:1 1M electrolyte. The solid line is W_j for the HNC/MSA theory, whereas the dashed and dotted lines are its MEP energy, V_j, and hard sphere, J_j, components, respectively. The dot-dashed and open circles are the URMGC and MC MEP energy, V_j, respectively. (a) is for $W_+(r=\text{IHP},\sigma_0)$, (b) is for $W_+(r=\text{OHP},\sigma_0)$, and (c) is for $W_-(r=\text{OHP},\sigma_0)$. Notice that the open circles in the figure, from left to right, are for $z_M = -8,-6,-4,-2,0,+2,+4,+6,+8$.

but beyond the OHP the field is cancelled monotonically since there is no ionic-size entropic contributions.

Figure 7 presents the HNC/MSA potential of the mean force $W_j(r)$ at the Helmholtz planes as functions of the macroion surface charge density σ_0, i.e., $W_j(\text{IHP},\sigma_0)$ and $W_j(\text{OHP},\sigma_0)$. As pointed out in Eq. (8), $W_j(r)$ can be expressed as the sum of the MEP energy, $V_j(r) \equiv e z_j \psi(r)$, and the entropic term, $J_j(r)$, where we have dropped the subindex M for simplicity. Note that in the graphs, these energy terms are in units of the thermal energy $k_B T$. Also included in Fig. 7 are the MC and URMGC results for $V_j(r)$ at the IHP and OHP. As it is usual in the analysis of the $\psi_{\text{IHP}}(\sigma_0)$ and $\psi_{\text{OHP}}(\sigma_0)$ functions, the colloidal charge is specified here in terms of the surface density $\sigma_0 (= z_M e/(\pi D_M^2))$. The reader can easily pass from σ_0 to z_M if realizes that the symbols

(open circles) in the figure, from left to right, correspond to the sequence of integer valences $z_M=-8,-6,-4,-2,0,+2,+4,+6,+8$.

The potential of mean force $W_+(\mathrm{IHP})=W_{j=+}(r'=D_+/2)$ is the necessary energy to bring a positive ion from infinity to the contact with the macroion of charge σ_0. Clearly, $W_+(\mathrm{IHP})<0$ for a macroion of negative charge in a size and charge symmetric electrolyte, i.e., there is an attractive energy. By symmetry, the same applies to negative ions when the charge of the macroion is positive; for $\sigma_0=0$ both type of ions will experience an attractive energy because the corresponding RDFs at contact are greater than one. This later entropic effect will persist [i.e., $W_+(\mathrm{IHP})<0$ for $\sigma_0\leq 0$] up to a critical positive charge density σ_c where $W_+(\mathrm{IHP})=0$. Accordingly, in Fig. 7(a) we observe that in the HNC/MSA approach, our size-asymmetric electrolyte displays the condition $W_+(\mathrm{IHP})<0$, even for a region of $\sigma_0>0$, from where we find that $W_+(\mathrm{IHP})\neq 0$ for $\sigma_0=0$. From the same graph it is clear that this is due to the entropic contribution, $J_+(\mathrm{IHP})$, i.e., because the ions adsorbed to the macroparticle's surface increase the accessible volume. On the other hand, $V_+(\mathrm{IHP})=ez_+\psi(\mathrm{IHP})$ is positive for a region of $\sigma_0<0$, i.e., there is an electrostatic repulsion of positive ions by a negative macroion. This repulsion is in part explained by Eqs. (5) and (8), where it is seen that the entropic or size effect is correlated with electrical effect and, on the other hand, can be understood in terms of the attraction of the positive small ions by the large negative ions adsorbed to the macroion's wall. This effect is also seen in the URMGC results where, for $\sigma_0<0$, the electrostatic energy $V_+(\mathrm{IHP})$ is less repulsive than that of HNC/MSA, which, in turn, is due to the fact that the HNC/MSA theory predicts a larger concentration of positive ions in the Helmholtz zone than the URMGC formalism. Finally, we wish to point out the excellent agreement between the HNC/MSA and MC data for $V_+(\mathrm{IHP})$.

In Fig. 7(b) we show $W_+(\mathrm{OHP})$. We still see a region of $\sigma_0>0$ where $W_+(\mathrm{OHP})<0$. The attraction, however, is lower because the OHP is further away than the IHP. On the other hand, the MC and HNC/MSA $V_+(\mathrm{OHP})$ are positive for a larger region of $\sigma_0<0$. This is because the adsorbed positive ions in the Helmholtz zone overcomes the electrical field due to the macroion and the adsorbed negative ions at the OHP. Notice that the URMGC result for $V_+(\mathrm{OHP})$ becomes negative as in Fig. 7(a). Here, again, this is because the HNC/MSA $V_+(\mathrm{OHP})$ is correlated with $J_+(\mathrm{OHP})$, which implies that because of the entropic effect already discussed above, in the HNC/MSA result there are more positive ions adsorbed than in the URMGC theory.

In the Fig. 7(c) we have a strong adsorption of negative ions at the OHP not only for $\sigma_0>0$, as expected, but for large negative values of σ_0. We know that a larger ionic size implies greater adsorption to the surface because the system needs to push more large ions to the interface in order to gain accessible volume. The negative values of $V_-(\mathrm{OHP})$, for $\sigma_0<0$, are explained, as above, because of the adsorption of positive ions in the region between the IHP and the OHP.

A relevant quantity in theoretical and experimental studies of colloidal systems is the MEP; hence the simulation and theoretical MEPs at the Helmholtz planes as functions of σ_0 are plotted in Fig. 8. As it is usual in the analysis of the $\psi_{\mathrm{IHP}}(\sigma_0)$ and $\psi_{\mathrm{OHP}}(\sigma_0)$ functions, the colloidal charge is specified here in terms of the surface density $\sigma_0(=z_M e/(\pi D_M^2))$. In Figs. 8(a) and 8(b), we observe that the $\psi_{\mathrm{IHP}}(\sigma_0)$ and $\psi_{\mathrm{OHP}}(\sigma_0)$ curves for the three approaches, namely, MC, HNC/MSA, and URMGC, display an increasing monotonic behavior and positive PZCs. Besides, the simulations and theories predict *the existence of intervals of negative colloidal charges near the point of zero charge for which the potentials at the IHP and OHP can be positive*, i.e., where the conditions $\sigma_0\psi_{\mathrm{IHP}}<0$ and $\sigma_0\psi_{\mathrm{OHP}}<0$ are accomplished. As it is indicated by Eq. (7), these attributes of ψ_{IHP} and ψ_{OHP} can be inferred, of course, from the comportment of the IC or better from the function $P(r)/r^2$ (which is basically the local mean electrostatic field around the macroparticle).

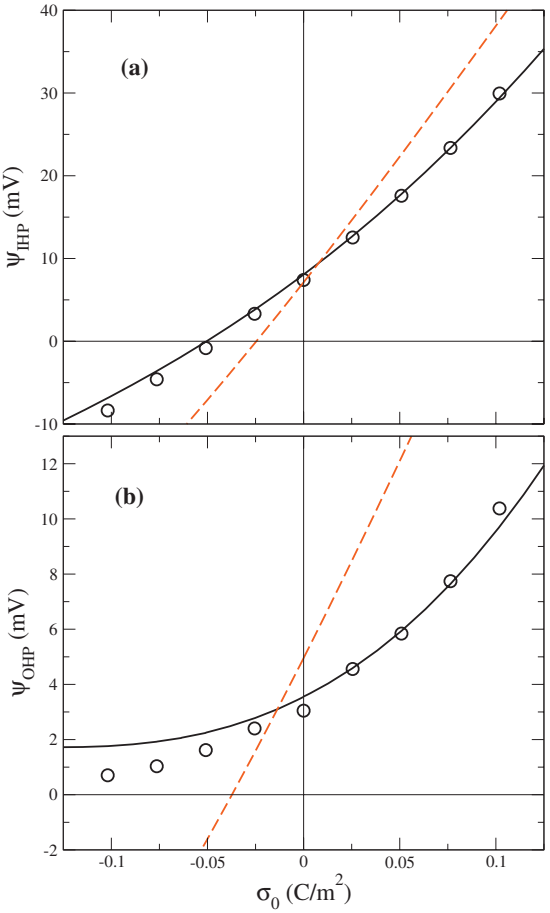

FIG. 8. MEP at the Helmholtz planes as functions of the surface charge density of a macroion immersed in a size-asymmetric 1:1 1*M* electrolyte. The open circles and solid and dashed lines correspond to simulations and the HNC/MSA and URMGC theories, respectively. In (a) the MEP at the IHP is plotted, and in (b) the same is done for the MEP at the OHP.

In connection with electrophoresis experiments and depending on the location of the shear plain, our potential-charge results suggest two possible scenarios. If the sign of the electrophoretic mobility, μ, were associated to the sign of the potential ψ_{IHP}, our treatment of the size-asymmetric EDL would predict a reversed colloidal mobility very near to the point of zero charge on the negative side. We recall that a negatively charged macroion would in principle move to the

anode. Hence, accordingly with our results, if the shear plane is at the macroion-cation contact value, the slightly charged macroion could move to the cathode (in the Smoluchowski approach to the mobility[2]). If the sign of μ were associated to the sign of the potential ψ_{OHP}, our MC and HNC/MSA study would foresee the negative macroion moving to the cathode (reversed mobility) for a wider range of macroion's negative charges. In addition, the ψ_{OHP} in Fig. 8(b) resembles a situation reported in Fig. 2b of Ref. 58 by Johnson *et al.*, where the zeta potential measurements of α-alumina in presence of $1M$ $LiNO_3$ are plotted as a function of pH. In those results, the zeta potential is always positive in a wide interval of pH that encompasses the point of zero charge, which parallels our results in Fig. 8(b). This would indicate that such positive values of the zeta potential are due in part to the preferential adsorption of one of the species (Li^+), which in turn should be induced by the ionic size asymmetry, as deduced from our survey of the SEDL. Although other complex mechanisms are into play in these kind of experiments,[59,56,95,96] our size-asymmetric model seems to capture adequately relevant phenomena occurring in real systems, and hence it could be considered as a basic representation of the EDL to which further improvements (as van der Waals dispersion forces or more sophisticated chemical mechanisms) can be incorporated in order to predict experimental data more accurately.

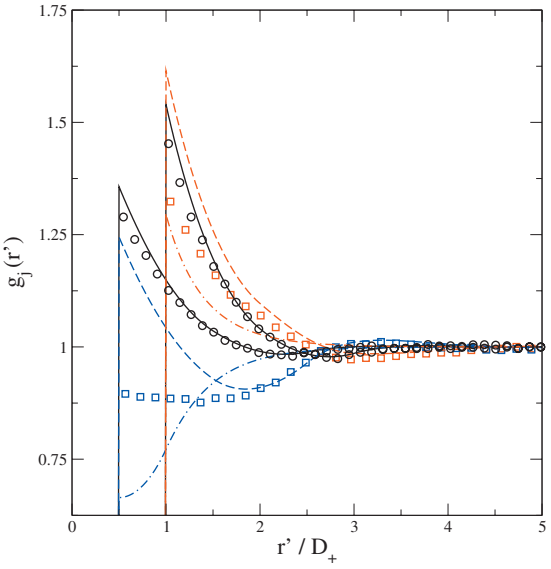

FIG. 9. RDFs of a size-asymmetric binary mixture of hard spheres and a size-asymmetric 2:2 electrolyte, both at a $0.5M$ concentration, around an uncharged ($z_M=0$) macroparticle as a function of the distance to the surface of the colloid. The small hard spheres have the same diameter as that of the cations, $D_1=D_+$, and the large hard spheres diameter is the same as that of the anions, $D_2=D_-$. The open circles correspond to MC simulations of the size-asymmetric mixture of hard spheres, and the open squares represent the MC data of the size-asymmetric divalent electrolyte. The solid lines are associated to the asymmetric mixture of hard spheres in the HNC/MSA approach. The dashed and dot-dashed lines are the HNC/MSA and URMGC results for the 2:2 size-asymmetric salt, respectively.

B. Divalent size-asymmetric electrolytes

We proceed to investigate the properties of the EDL for a macroion immersed in a 2:2 salt, i.e., for systems with stronger charge correlations. As it will be shown, many of the findings reviewed in the prior section devoted to univalent electrolytes are also present, in an enhanced way, for the case of divalent ions. As before, we examine first the EDL at the point of zero charge and later we ponder instances with charged macroparticles. In what follows, we consider EDL systems formed by a colloid and a bath of a 2:2 $0.5M$ electrolyte, with the same diameters as specified in the earlier section.

The simulation, HNC/MSA, and URMGC radial distributions of divalent ions around a macroparticle with $z_M=0$ are included in Fig. 9. There we have incorporated the MC and HNC/MSA pair correlation functions for the associated hard-sphere mixture (uncharged ions). Again, the idea is to exemplify how the Coulombic correlations modify the structure of the pure hard-sphere fluid in order to gain some insight into the relative importance of the entropic and charge correlations. From the direct contrast between the simulation RDFs of hard spheres and ions, we observe that the charge effects are very strong, completely modifying the accumulation of the smaller species around the macroparticle. In fact, the changes in the MC $g_j(r')$ of divalent ions with respect to the RDFs of hard spheres are bigger than those occurring in univalent systems (compare Figs. 1 and 9). For the simulations of 2:2 electrolytes, the impact of the valence is much more important for the smaller ionic species, where we observe that the corresponding contact population depletes so much that the concentration of cations near the surface is below the bulk value. In a lesser degree this dewetting effect is also present in the anion profiles, as compared to the 1:1 case. This overall dewetting of the non-charged surface is due to the electrostatic self-interaction energy of the system. A similar dewetting has been reported in a recent study of the planar EDL for size-asymmetric 1:1, 1:2, and 1:3 salts,[70] with the multivalent ions corresponding to the smaller species. In that work it was found that the amount of small cations in the proximities of a neutral plane decreased as long as the electrostatic coupling (i.e., the valence) was heightened, being our results consistent with such behavior. On the other hand, in Fig. 9 we can appreciate that the HNC/MSA results for hard spheres compare well with the simulations, whereas for the divalent case this formalism overestimates the MC data for the two ionic species. Furthermore, HNC/MSA fails to describe the correct tendency for the RDF of big anions, predicting an increase in such function with respect to the corresponding RDF of the larger hard spheres, which is clearly not the behavior seen in the MC data. The tendency for the RDFs of small hard spheres and small cations is correct, as compared to MC, although HNC/MSA fails to predict a large dewetting. Special note must be taken of the very low URMGC concentration of small ions in the Helmholtz zone, which, analogously to the univalent case, will determine the weak intensity of the CR and OC phenomena for 2:2 systems in this theory.

The strong difference in the adsorption of the little ions to the uncharged macroion between the HNC/MSA theory and MC results is a shortcoming of the HNC/MSA theory, which underestimates the bulk ion-ion correlations. Such

correlations are responsible for the dewetting phenomena in an electrolyte next to an uncharged wall. The mentioned shortcoming is also responsible for the consistent overestimation of the HNC/MSA contact value of the RDFs with respect to the MC results, only that now, since the macroion-ion electrostatic interaction has been turned off, through the HNC closure (remember that in our HNC/MSA theory, the macroion-ion interactions are taken through the HNC closure, whereas the ion-ion interactions are taken through the MSA closure), this effect is enhanced. Although, as pointed out before, all these interactions are interconnected in a very fundamental way in the general formalism of the IEs theory, to give the effective macroion-ion and ion-ion correlations. In particular, of course, this is the case in the HNC/MSA theory. Therefore the large and small ions adsorption to the uncharged macroion is strongly ruled by entropy, in the HNC/MSA theory, which of course implies a larger adsorption to the macroion of the large ions. The ion-ion correlations are of course also present and shown in our MC results. In the MC case the adsorption of the large negative ions is lower than for the corresponding hard-sphere profile due to the ion-ion repulsion. To understand the very low adsorption of the positive little ions one has to take into account the lower entropic effect, due to their smaller size, and the electrostatic attraction of the bulk: remember that for a symmetric electrolyte next to an uncharged surface there is dewetting of positive and negative ions, due precisely to the self attraction of the bulk fluid. This is in fact another important consequence of the ionic size-asymmetry, where it is clearly seen the entropic contribution to the EDL. On the other hand, this also explains the good results for the unsymmetrical hard-sphere mixtures in the HNC/MSA theory.

The simulation and theoretical ionic distributions of the divalent salt yield the accumulated charge and MEP given in Fig. 10 and its inset. As it was detected in the monovalent situation, the ionic size asymmetry promotes an adsorbed layer of charge and the concomitant existence of an EDL for a non-charged surface (see Fig. 9), as well as a nonzero MEP at (and between) the Helmholtz planes. The adsorbed charges, up to the OHP, are $\approx 2.6e$, $3.3e$, and $2.0e$ for MC, HNC/MSA, and URMGC, respectively, which are smaller than those observed for the 1:1 salt. This is because the higher molar concentration of the 1:1 electrolyte, which implies a higher entropic energy. In turn, contrasted with MC, the MEP within the Helmholtz planes is overestimated by HNC/MSA and underestimated by URMGC. Globally we see that the performance of HNC/MSA and URMGC is very similar to that displayed for the monovalent salt, with a better qualitative similitude between HNC/MSA and the simulations. For URMGC the $P(r')$ and $\psi(r')$ profiles evidence the restriction of all the size asymmetry and hard-core effects to happen uniquely in the Helmholtz zone. Notice that despite the poor agreement of the RDF of HNC/MSA with our MC data, there is a reasonable good agreement for the corresponding $P(r')$ and $\psi(r')$.

The MC and theoretical RDFs, IC, and MEP curves corresponding to the divalent electrolyte and two values of the colloidal charge, namely, $z_M=-4$ and $z_M=4$, are plotted in Figs. 11 and 12. When $z_M=-4$ [Fig. 11(a)], there is a strong

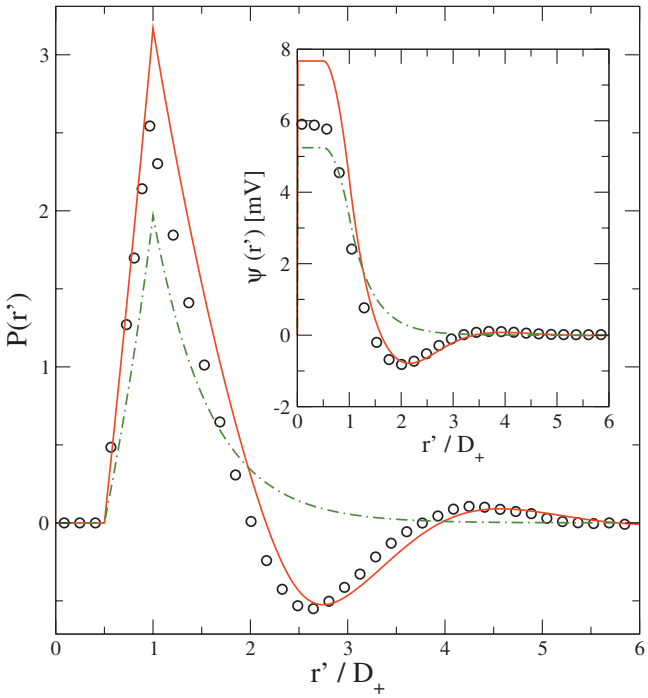

FIG. 10. IC (main panel) and MEP (inset) of a size-asymmetric 2:2 0.5*M* electrolyte around an uncharged ($z_M=0$) macroparticle as a function of the distance to the surface of the colloid. The open circles, solid, and dot-dashed lines are associated to the MC, HNC/MSA, and URMGC data, respectively.

adsorption of counterions inside the Helmholtz planes, accompanied by an important depletion of coions, particularly for MC and HNC/MSA. Besides, it is worth noticing that very close to the OHP the concentration of coions is smaller than that of counterions [compare with Fig. 3(a)], which imply that at these distances the repulsion forces between the macroion and the coions are far from being screened, as a consequence of a smaller entropic driving force for the 2:2 0.5*M* case. When $z_M=4$ [Fig. 11(b)] and despite of the intense electrostatic repulsion, the MC, HNC/MSA, and URMGC concentrations of the small coions close to the IHP turn out to be small but different from zero, effectively increasing the charge of the macroion and therefore enhancing the counterions concentration near the OHP.

In Fig. 12 we present the ICs and MEPs for the divalent salt and macroion valences $z_M=-4$ and $z_M=4$. For $z_M=-4$ [panel (a)], the ICs of MC and HNC/MSA exhibit CR in the Helmholtz zone, but the maximum CRs are outside that region (at $r'/D_+\approx 1.5$ and $r'/D_+\approx 1.4$ for simulations and HNC/MSA, respectively). The corresponding MEPs, on the other hand, display a strong reversal, with the maximum potential being inside the Helmholtz planes (see inset). In the case $z_M=4$ [panel (b)], we see that the MC and HNC/MSA IC profiles present OC, followed by alternate oscillations of decreasing amplitude, whereas the associated MEPs (in the inset) decay in a fluctuating manner to zero. This observation of OC in the computer experiments of divalent systems complements our previous findings for univalent salts and, thus, consolidates our simulation proof of OC as a genuine feature of size-asymmetric PM EDLs.

A simultaneous analysis of all the structural information for divalent systems contained in Figs. 11 and 12 show that

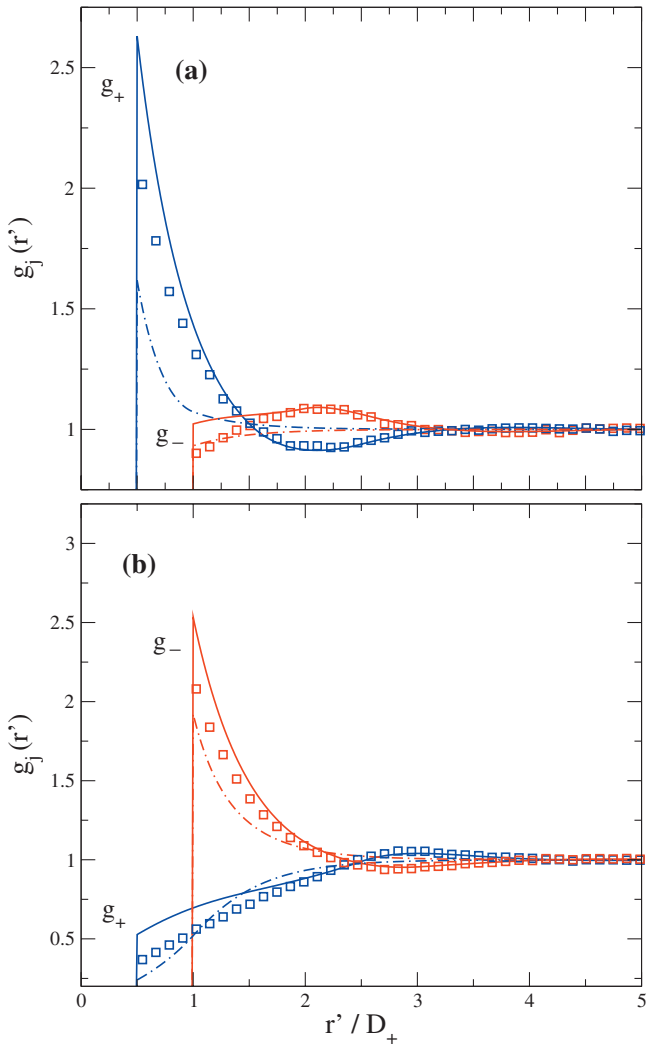

FIG. 11. RDFs of a size-asymmetric 2:2 0.5*M* electrolyte around a charged macroion as a function of the distance to the surface of the colloid. In (a) $z_M=-4$, and in (b) $z_M=4$. The open squares, solid, and dot-dashed lines represent the MC, HNC/MSA, and URMGC results, respectively.

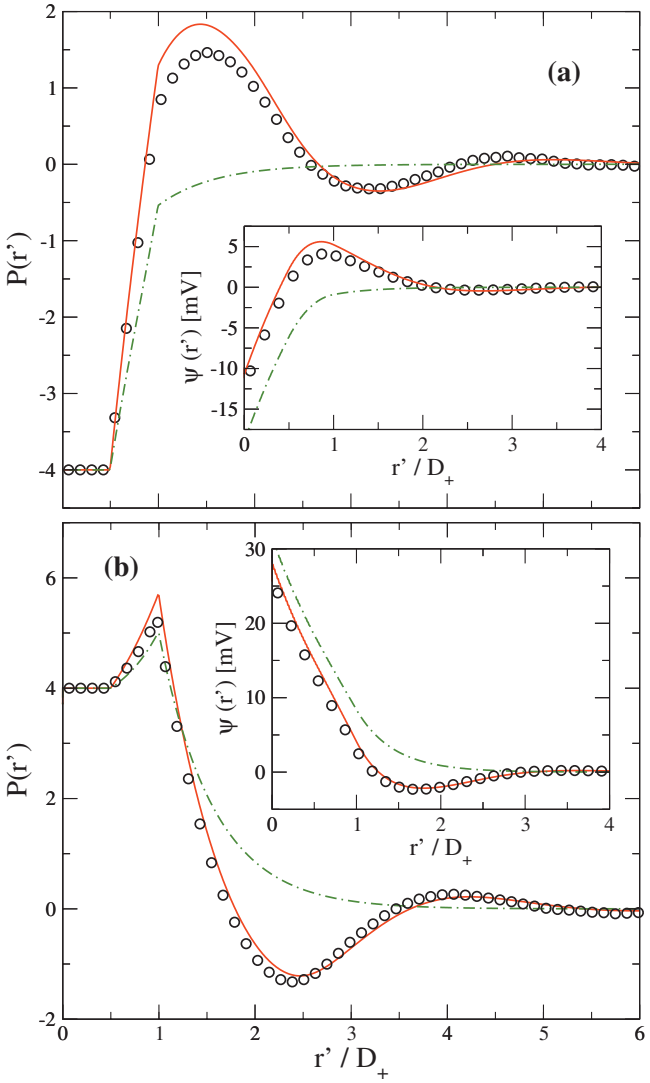

FIG. 12. IC (main panels) and MEP (insets) of a size-asymmetric 2:2 0.5*M* electrolyte around a charged macroion as a function of the distance to the surface of the colloid. In (a) $z_M=-4$, and in (b) $z_M=4$. The open circles, solid, and dot-dashed lines correspond to the MC, HNC/MSA, and URMGC data, respectively.

the HNC/MSA theory follows closely the MC data, whereas the URMGC approach exhibits notable differences with respect to the simulations. From these figures it is also verified that in the URMGC description of the EDL there is a confinement of the steric-related phenomenology (e.g., CR, OC, and the nonmonotonic character of the structural functions) within the Helmholtz zone.

Figure 13 portrays the MC and HNC/MSA ICs for varying $z_M(-8\leq z_M\leq 8)$ in order to analyze the evolution of the size asymmetry effects when the divalent systems depart from the point of zero colloidal charge. For $z_M<-2$ [Fig. 13(a)] the IC profiles of MC and HNC/MSA present CR, with the maximum located outside the Helmholtz zone. As the charge increases (toward $z_M=0$), the location of the peak of each curve shifts to shorter distances and eventually lands at the OHP (see Fig. 10). Further increase in z_M leads to the results plotted in Fig. 13(b), where the system displays OC, with a maximum intensity (i.e., $|P(r')-z_M|$) that decreases with the augment of the macroion's valence. Clearly, this is due to the fact that a larger z_M implies a large repulsion of the little positive ions, i.e., coions. This OC phenomenon only takes place in between the Helmholtz planes, and it is followed by a first region of CR. At the limiting valence $z_M\approx 16$ OC virtually disappears; meanwhile the CR beyond the OHP continues to exist with an increasing magnitude. All these characteristics of $P(r')$ for $z_M>0$ are equally described for both the simulations and HNC/MSA. At this point we wish to point out that another confirmation of OC, by molecular dynamics simulation for size unsymmetrical, multivalent electrolytes, next to a charged plate, has been recently reported.[72] Our results here, for divalent, size unsymmetrical electrolytes, as a function of the macroparticle charge [Fig. 13(b)], support the OC mechanism presented previously for a macroion solution next to a charged wall.[38] *The complete development of the* $P(r')$ for 2:2 electrolytes and $-8\leq z_M\leq 8$ reveals a passage from CR to OC. This crossover at $z_M=0$ is due uniquely to the size asymmetry of the salt ions, as the change in sign of z_M merely inverts the role of the anions and cations (as coions or counterions).

Therefore, in the present investigation it has been found

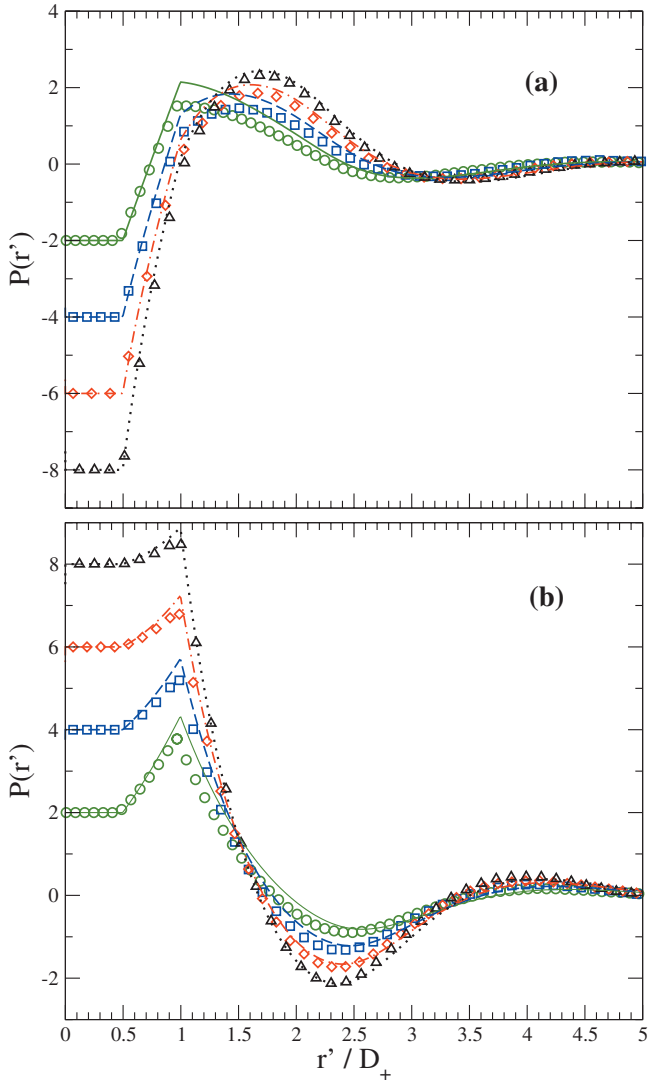

FIG. 13. IC of a size-asymmetric 2:2 0.5*M* electrolyte around a charged macroion as a function of the distance to the surface of the colloid. In (a) the open circles, squares, diamonds, and triangles correspond to MC simulations for $z_M=-2,-4,-6,-8$, respectively, and in (b) are associated to $z_M=2,4,6,8$, respectively. In (a) the solid, dashed, dot-dashed, and dotted lines correspond to HNC/MSA results for $z_M=-2,-4,-6,-8$, respectively, and in (b) are associated to $z_M=2,4,6,8$, respectively.

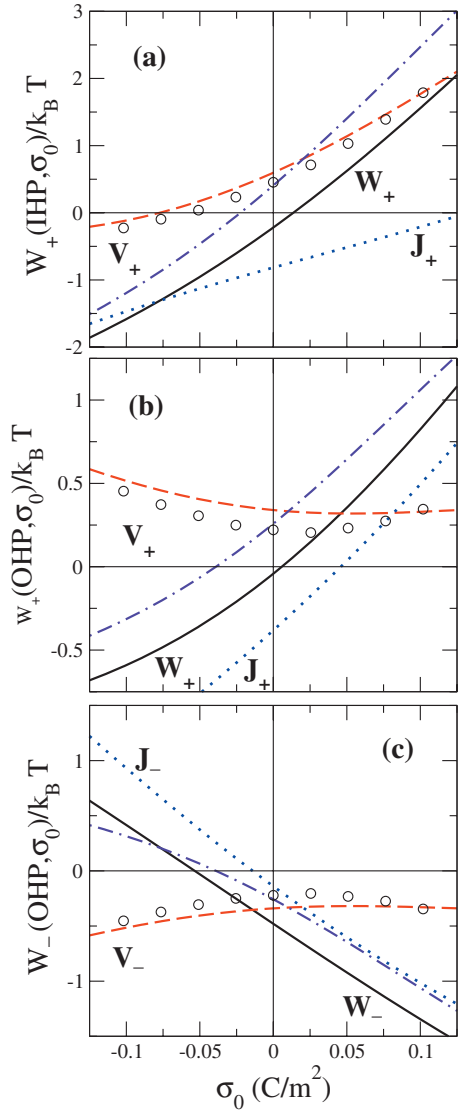

FIG. 14. Potential of mean force, W_j, of an ion of species j at the IHP and OHP as a function of the macroparticle surface charge density, σ_0, for a size-asymmetric 2:2 0.5*M* electrolyte. The solid line is W_j for the HNC/MSA theory, whereas the dashed and dotted lines are its MEP energy, V_j, and hard sphere, J_j, components, respectively. The dot-dashed and open circles are the URMGC and MC MEP energy, V_j, respectively. (a) is for $W_+(r=\text{IHP},\sigma_0)$, (b) is for $W_+(r=\text{OHP},\sigma_0)$, and (c) is for $W_-(r=\text{OHP},\sigma_0)$. Notice that the open circles in the figure, from left to right, are for $z_M=-8,-6,-4,-2,0,+2,+4,+6,+8$.

that the CR and OC observed near the point of zero charge are mainly caused by entropic contributions coming from the size-asymmetric nature of the electrolyte ions. This strong entropic contribution is also responsible for the crossing points in the IC curves and the corresponding local inversion of the derivative of the IC regions [see Eq. (12) and the discussion below it] for the different values of z_M shown in Figs. 13(a) and 13(b). However, when z_M is increased, the CR [Fig. 13(a)] and OC [Fig. 13(b)] in the Helmholtz zone disappear, and only CR persists. This remaining CR beyond the OHP comes from the interplay between excluded volume and electrostatic correlations, and thus, it is not exclusive of a size-asymmetric model. That is the reason why CR has been already reported in many studies of the RPM EDL, in which the excluded volume effects are also consistently taken into account.[20] Accordingly, EDL theories for *genuine* punctual ions and uniformly charged surfaces do not predict CR at all. The corresponding sequence $(-8\leq z_M\leq 8)$ of URMGC ICs for 2:2 electrolytes has a similar qualitative behavior as that shown for the 1:1 case (see Fig. 6).

Figure 14 presents the HNC/MSA potential of mean force $W_j(r)$, the mean electrostatic energy $V_j(r)$, and the entropic term $J_j(r)$ at the Helmholtz planes, as functions of σ_0, for the divalent electrolyte. The MC and URMGC results for $V_j(r)$ at the IHP and OHP are also included.

The trends observed in Figs. 14(a) and 14(b) for HNC/MSA are similar to those in Figs. 7(a) and 7(b). The main differences reside in a reduction in the range of $\sigma_0>0$ for which $W_+(\text{IHP})<0$ and $W_+(\text{OHP})<0$ and a nonmonotonic behavior of the $V_+(\text{OHP})$, i.e., that $V_+(\text{OHP})$ increases when $|\sigma_0|$ increases. This nonmonotonic behavior of $V_+(r)$ at the OHP for $\sigma_0<0$ is due to the excess of positive ions adsorbed

to the macroion in the Helmholtz zone, driven by the entropic force. In Figs. 11–13 we see the effect of the enhanced entropic force when comparing the HNC/MSA and URMGC theories, i.e., the counterion adsorption is far larger in the HNC/MSA and MC results than in the URMGC.

On the other hand, the reduction in the interval of $\sigma_0>0$, with respect to the 1:1 case, for which $W_+(\mathrm{IHP})<0$ and $W_+(\mathrm{OHP})<0$ is due to both a less entropic force for the now little coions and a higher electrostatic repulsion since now they are divalent. Both effects, the nonmonotonic behavior of $V_+(\mathrm{OHP})$ and the reduction in the interval of $\sigma_0>0$ for which the potentials of mean force of cations at the IHP and OHP are negative, as compared to the 1:1 results in Fig. 7, are originated, on the one hand, by the higher energy contribution in the divalent case and by the higher entropic contribution in the monovalent case ($\rho_{\pm}=1M$ in the 1:1 electrolyte and $\rho_{\pm}=0.5M$ in the 2:2 salt). As we have discussed before, a higher electrolyte concentration implies a higher entropic ionic adsorption, and a higher ionic charge increases the energy contribution. Therefore, the entropy-energy balance is dominated by the energy for the 2:2 electrolyte, as compared to the 1:1 salt.

Figures 14(a) and 14(b) present the MEP energy, $V_j(r)\equiv ez_j\psi(r)$ of MC, HNC/MSA, and URMGC at the Helmholtz planes ψ_{IHP}, and ψ_{OHP}, as functions of σ_0. Notice that the MEP is the MEP energy divided by the ionic charge. At the IHP, all the approaches exhibit a MEP that is monotonic, a positive zero-charge potential, and a negative σ_0^{crit} such that $\psi_{\mathrm{IHP}}>0$ for $\sigma_0^{\mathrm{crit}}<\sigma_0<0$, just like in the monovalent systems. From panel (b) we also find that ψ_{OHP} is also monotonic for URMGC. In contrast to the monovalent case, however, ψ_{OHP} from MC and HNC/MSA is nonmonotonic and displays a minimum at a positive σ_0^{min}. This augment of ψ_{OHP} when σ_0 decreases below σ_0^{min} suggests that there could be experimental systems in which the reverted electrophoretic mobility always increases its magnitude.

The trends of these MEPs can be explained in terms of the corresponding IC profiles (see Fig. 13), as discussed previously in the context of monovalent electrolytes. In particular, the concavity of ψ_{OHP} for MC and HNC/MSA can be explained by observing in Fig. 13(b) the behavior of the integral of $P(r)/r^2$ between the first two consecutive electroneutral points of $P(r)$ and noting that the absolute value of these negative areas decreases when z_M diminishes. Thus, for $\sigma_0\geq 0$, the area from the OHP to the first electroneutral point is positive and larger than the negative area between the first and second electroneutral points [see Fig. 13(b)]. Since the difference between these two contributions to the ψ_{OHP} increases with σ_0, this explains the positive value of ψ_{OHP} and its increasing behavior. An analogous argument explains the MC and HNC/MSA trends observed when $\sigma_0<0$ [Fig. 13(a)] despite the disappearance of the maximum CR at the OHP when z_M decreases.

For MC and HNC/MSA, the behavior of the derivative of ψ_{OHP} observed in Fig. 14(b) for $\sigma_0<0$ implies that (see related discussion in Fig. 15 below) as

$$\frac{\partial\psi(\sigma_0,r'=D_+)}{\partial\sigma_0}<0. \tag{13}$$

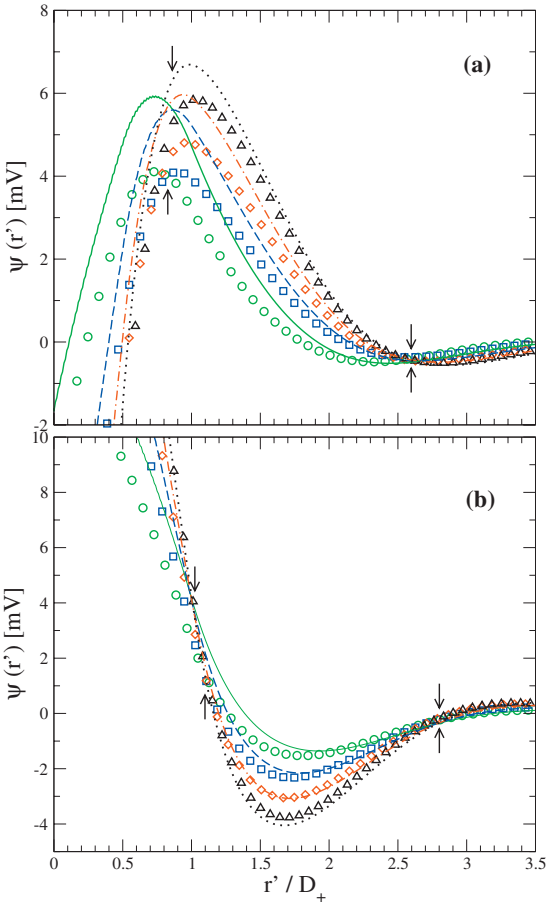

FIG. 15. MEP of a size-asymmetric 2:2 $0.5M$ electrolyte around a charged macroion as a function of the distance to the surface of the colloid. In (a) the open circles, squares, diamonds, and triangles correspond to MC simulations for $z_M=-2,-4,-6,-8$, respectively, and in (b) are associated to $z_M=2,4,6,8$, respectively. In (a) the solid, dashed, dot-dashed, and dotted lines correspond to HNC/MSA results for $z_M=-2,-4,-6,-8$, respectively, and in (b) are associated to $z_M=2,4,6,8$, respectively.

Since ionic size and size asymmetry are evidently important in real highly coupled electrokinetic systems, these last result suggest that the interpretation of the zeta potential ζ in electrokinetic experiments must be done carefully because there is the possibility of decreasing ζ for increasing σ_0 and vice versa. The occurrence of these nonmonotonic effects in the potential is clearly precluded in the PB-based interpretation of the experimental measurements, as evidenced in the present study.

By observing the MC and HNC/MSA $\psi(r)$ in Fig. 15 for varying z_M, it is also detected that the maxima of the $\psi(r)$ are located between the IHP and OHP. These maxima correspond to distances at which $P(r)=0$ or $E(r)=-[d\psi(r)/dr]=0$, which means that for the divalent ions the DL becomes more compact due to the great amount of positive ions adsorbed between the IHP and OHP. Thence the increasing of $\psi(r)$ as σ_0 decreases is a consequence of the CR at the OHP, which is consistent with our above discussion. This nonlinear behavior of $P(r)$ and $\psi(r)$, as a function of z_M, indicates a corresponding possible nonlinear response of the macroion to external electrical fields in electrophoretic studies.[13,14]

V. SUMMARY AND CONCLUSIONS

In this paper the size-asymmetric EDL of 1:1 and 2:2 salts around a slightly charged spherical macroparticle was studied by assuming the PM of an electrolyte as a representation of the ionic bath and using MC simulations and the HNC/MSA IE in order to calculate the corresponding properties of the model system. Therefore, in the simulation and HNC/MSA IE, the important ionic size and size asymmetry effects have been fully incorporated through the consistent consideration of the colloid-ions and ion-ion interactions. Additionally, the possible consequences of a partial treatment of such excluded volume and size asymmetry contributions in the properties of the SEDL were assessed via the comparison with the predictions of the classic URMGC theory for spherical geometry. In the semipunctual URMGC formalism, the finite nature of the ions is considered only through the use of two different distances of closest approach between the colloid and counterions and colloid and coions. Our MC data evince that the finite size and size asymmetry of the ionic species near a barely charged colloid produce remarkable phenomena, such as CR, OC, the existence of PZCs, and of a zero charge EDL, as well as the possibility of oscillations in the ionic densities and of sign alternacy in the MEP. The simulations also show that the extent of all these features is intimately linked to the ability of the smallest ions to penetrate the Helmholtz zone. Importantly, in this report we present the first simulation corroboration of OC in the PM EDL (i.e., of the increment in the native colloidal charge prompted by an anomalous adsorption of coions), a peculiarity originally predicted by Jiménez-Ángeles and Lozada-Cassou[38] in a more complex EDL system.[72] Here it is evidenced that close to the point of zero charge, OC is a direct consequence of the size asymmetry of the ions. On the whole, the HNC/MSA results coincide with the simulations, then providing an essentially correct picture of the size-asymmetric SEDL near the point of zero charge. In contrast, URMGC disagrees quantitatively and qualitatively with the MC trends in most of the situations examined here. Notably, and due to its inconsistent treatment of the hard-core and electrostatic correlations, URMGC exhibits a spatial localization of all its "ionic size" and size asymmetry effects within the zone delimited by the IHP and OHP. One of the most characteristic sequels of the full incorporation of the ionic correlations in all the extension of the EDL and not only in the Helmholtz zone is the occurrence of a nonmonotonic behavior in the ionic concentration, charge density, and MEP profiles of MC and HNC/MSA in all the EDL. In this respect, the existence of spatial regions in which the IC and MEP present a nonuniform comportment with respect to the variation in the colloidal charge proves its relevance for the understanding of the potential-charge relationship at the Helmholtz planes. In particular, such "nonuniform" regions serve to explain the existence of a singular minimum in the $\psi_{\mathrm{OHP}}-\sigma_0$ curve for divalent salts.

Among the results not reported before and which are a direct consequence of the ionic size asymmetry are the counterintuitive attraction of positive little ions by a positively charged macroparticle or the attraction of large negative ions by a negatively charged macroion, both near the point of zero charge. Also interesting is that these effects are more significant for 1:1 electrolytes than for 2:2, as a result of a shift of the entropy-energy balance toward the entropy contribution for the 1:1 electrolyte, which has lower ionic charge and higher electrolyte concentration.

The plausible identification between the well-known zeta potential and the MEP around the Helmholtz zone, which is a usual hypothesis in the interpretation of electrophoretic mobility measurements, leads us to suggest several phenomena (e.g., the presence of an anomalous sign in the zeta potential and the occurrence of increased reversed mobilities), which could be the objectives of future experimental protocols. As a first attempt in this direction, we have pointed out the consistency between our results and some experimental data of electrokinetic mobilities for α-alumina particles.[58] The eventual confirmation in the laboratory of any of the theoretical predictions presented in this work (for example, CR and OC) by means of some electrokinetic or static technique could indicate the pertinence of our simple PM-based representation of the size-asymmetric SEDL as a starting point to develop more faithful descriptions of real colloidal systems, either in equilibrium or under external fields. Finally, and in relation with this, the rich phenomenology discussed in the present communication that arises from both the ionic size and size asymmetry effects puts a word of caution about the possible usage of the PB viewpoint and other contingent formalisms, such as the so-called standard electrokinetic model,[97] outside their range of applicability.

Although beyond the scope of this paper, clearly if the ionic size-asymmetry ratio is large enough, OC and the like-charged particles attractions will be present *even for wall charges far away from the point of zero charge*. We believe that this has not been noted in the literature and may have important consequences in several applications, e.g., drug delivery, self-assembly, polymer coating, and colloidal stability. In general, OC will be enhanced depending also on ionic charge and concentration and macroion's charge and geometry. Details of these effects will be reported elsewhere.

ACKNOWLEDGMENTS

This work was supported in part by Consejo Nacional de Ciencia y Tecnología (CONACYT, México) through Grant Nos. CB-2006-01/58470 and C01-47611 and PROMEP. E.G.-T. thanks Centro Nacional de Supercómputo of Instituto Potosino de Investigación Científica y Tecnológica for the computing time in the Cray XD1 and IBM E-1350 machines. G.I.G.-G. acknowledges postdoctoral fellowships from CONACYT and Instituto Mexicano del Petróleo.

[1] K. S. Schmitz, *Macroions in Solution and Colloidal Suspension* (VCH, New York, 1993).
[2] P. C. Hiemenz and R. Rajagopalan, *Principles of Colloid and Surface Chemistry* (Marcel-Dekker, New York, 1997).
[3] R. J. Hunter, *Foundations of Colloid Science* (Clarendon, Oxford, 1987).
[4] N. E. Hoskin and S. Levine, Philos. Trans. R. Soc. London, Ser. A **248**, 449 (1956).
[5] J. E. Sánchez-Sánchez and M. Lozada-Cassou, Chem. Phys. Lett. **190**, 202 (1992).

[6] G. I. Guerrero-García, E. González-Tovar, M. Lozada-Cassou, and F. de J. Guevara-Rodríguez, J. Chem. Phys. **123**, 034703 (2005).
[7] U. P. Strauss, N. L. Gershfeld, and H. Spiera, J. Am. Chem. Soc. **76**, 5909 (1954).
[8] G. S. Manning, Q. Rev. Biophys. **11**, 179 (1978).
[9] M. Elimelech and C. R. O'Melia, Environ. Sci. Technol. **24**, 1528 (1990).
[10] A. Martín-Molina, M. Quezada-Pérez, F. Galisteo-González, and R. Hidalgo-Álvarez, J. Chem. Phys. **118**, 4183 (2003).
[11] M. Quesada-Pérez, E. González-Tovar, A. Martín-Molina, M. Lozada-Cassou, and R. Hidalgo-Álvarez, Colloids Surf., A **267**, 24 (2005).
[12] E. Gonzales-Tovar, M. Lozada-Cassou, and D. Henderson, J. Chem. Phys. **83**, 361 (1985); **87**, 5581 (1987).
[13] M. Lozada-Cassou, E. González-Tovar, and W. Olivares, Phys. Rev. E **60**, R17 (1999).
[14] M. Lozada-Cassou and E. González-Tovar, J. Colloid Interface Sci. **239**, 285 (2001).
[15] M. Tanaka and A. Y. Grosberg, Eur. Phys. J. E **7**, 371 (2002).
[16] K. Besteman, M. A. G. Zevenbergen, H. A. Heering, and S. G. Lemay, Phys. Rev. Lett. **93**, 170802 (2004).
[17] K. Besteman, M. A. G. Zevenbergen, and S. G. Lemay, Phys. Rev. E **72**, 061501 (2005).
[18] F. H. J. van der Heyden, D. Stein, K. Besteman, S. G. Lemay, and C. Dekker, Phys. Rev. Lett. **96**, 224502 (2006).
[19] M. Tanaka and A. Y. Grosberg, J. Chem. Phys. **115**, 567 (2001).
[20] T. Terao and T. Nakayama, Phys. Rev. E **63**, 041401 (2001).
[21] M. Deserno, F. Jiménez-Ángeles, C. Holm, and M. Lozada-Cassou, J. Phys. Chem. B **105**, 10983 (2001).
[22] F. Jiménez-Ángeles and M. Lozada-Cassou, J. Chem. Phys. **128**, 174701 (2008).
[23] L. B. Bhuiyan, C. W. Outhwaite, and S. Levine, Mol. Phys. **42**, 1271 (1981).
[24] C. W. Outhwaite and L. B. Bhuiyan, J. Chem. Soc., Faraday Trans. 2 **79**, 707 (1983).
[25] M. Lozada-Cassou, R. Saavedra-Barrera, and D. Henderson, J. Chem. Phys. **77**, 5150 (1982).
[26] E. González-Tovar and M. Lozada-Cassou, J. Phys. Chem. **93**, 3761 (1989).
[27] R. Kjellander, S. Marčelja, R. M. Pashley, and J. P. Quirk, J. Chem. Phys. **92**, 4399 (1990).
[28] L. Mier-y-Teran, S. H. Sun, H. S. White, and H. T. Davis, J. Chem. Phys. **92**, 5087 (1990).
[29] C. N. Patra and S. K. Ghosh, J. Chem. Phys. **117**, 8938 (2002).
[30] D. Boda, D. H. W. R. Fawcett, and S. Sokolowski, J. Chem. Phys. **116**, 7170 (2002).
[31] G. M. Torrie and J. P. Valleau, J. Phys. Chem. **86**, 3251 (1982).
[32] V. Vlachy and A. O. J. Haymet, J. Chem. Phys. **84**, 5874 (1986).
[33] L. Degrève, M. Lozada-Cassou, E. Sánchez, and E. González-Tovar, J. Chem. Phys. **98**, 8905 (1993).
[34] L. Degrève and M. Lozada-Cassou, Mol. Phys. **86**, 759 (1995).
[35] H. Greberg and R. Kjellander, J. Chem. Phys. **108**, 2940 (1998).
[36] R. Messina, E. González-Tovar, M. Lozada-Cassou, and C. Holm, Europhys. Lett. **60**, 383 (2002).
[37] J. Lyklema, Colloids Surf., A **291**, 3 (2006).
[38] F. Jiménez-Ángeles and M. Lozada-Cassou, J. Phys. Chem. B **108**, 7286 (2004).
[39] M. Quesada-Pérez, E. González-Tovar, A. Martín-Molina, M. Lozada-Cassou, and R. Hidalgo-Álvarez, ChemPhysChem **4**, 234 (2003).
[40] S. L. Carnie, D. Y. C. Chan, D. J. Mitchell, and B. W. Ninham, J. Chem. Phys. **74**, 1472 (1981).
[41] V. Vlachy and D. A. McQuarrie, J. Chem. Phys. **83**, 1927 (1985).
[42] M. Lozada-Cassou and E. Díaz-Herrera, J. Chem. Phys. **92**, 1194 (1990).
[43] C. W. Outhwaite and L. B. Bhuiyan, Mol. Phys. **74**, 367 (1991).
[44] M. Lozada-Cassou, in *Fundamentals of Inhomogeneous Fluids*, edited by D. Henderson (Marcel-Dekker, New York, 1992).
[45] L. Yeomans, S. E. Feller, E. Sánchez, and M. Lozada-Cassou, J. Chem. Phys. **98**, 1436 (1993).
[46] E. González-Tovar, F. Jiménez-Ángeles, R. Messina, and M. Lozada-Cassou, J. Chem. Phys. **120**, 9782 (2004).
[47] Y. X. Yu, J. Z. Wu, and G. H. Gao, J. Chem. Phys. **120**, 7223 (2004).
[48] L. B. Bhuiyan, C. W. Outhwaite, and D. Henderson, J. Chem. Phys. **123**, 034704 (2005).
[49] F. Jiménez-Ángeles, R. Messina, C. Holm, and M. Lozada-Cassou, J. Chem. Phys. **119**, 4842 (2003).
[50] F. Jiménez-Ángeles, G. Odriozola, and M. Lozada-Cassou, J. Chem. Phys. **124**, 134902 (2006).
[51] T. Goel and C. N. Patra, J. Chem. Phys. **127**, 034502 (2007).
[52] A. Dukhin, S. Dukhin, and P. Goetz, Langmuir **21**, 9990 (2005).
[53] S. S. Dukhin and A. E. Yaroschuck, Kolloidn. Zh. **44**, 884 (1982).
[54] B. V. Derjaguin, S. S. Dukhin, and A. E. Yaroschuck, J. Colloid Interface Sci. **115**, 234 (1987).
[55] S. S. Dukhin, N. V. Churaev, V. N. Shilov, and V. M. Starov, Russ. Chem. Rev. **57**, 572 (1988).
[56] M. Colic, G. V. Franks, M. L. Fisher, and F. F. Lange, Langmuir **13**, 3129 (1997).
[57] M. Colic, M. L. Fisher, and G. V. Franks, Langmuir **14**, 6107 (1998).
[58] S. B. Johnson, P. J. Scales, and T. W. Healy, Langmuir **15**, 2836 (1999).
[59] S. B. Johnson, G. V. Franks, P. J. Scales, and T. W. Healy, Langmuir **15**, 2844 (1999).
[60] M. Manciu and E. Ruckenstain, Adv. Colloid Interface Sci. **105**, 63 (2003).
[61] R. Rahnemaie, T. Hiemstra, and W. H. van Riemsdijk, J. Colloid Interface Sci. **293**, 312 (2006).
[62] T. Hiemstra and W. H. V. Riemsdijk, J. Colloid Interface Sci. **301**, 1 (2006).
[63] J. P. Valleau and G. M. Torrie, J. Chem. Phys. **76**, 4623 (1982).
[64] L. B. Bhuiyan, L. Blum, and D. Henderson, J. Chem. Phys. **78**, 442 (1983).
[65] J. J. Spitzer, J. Colloid Interface Sci. **92**, 198 (1983).
[66] A. F. Khater, D. Henderson, L. Blum, and L. B. Bhuiyan, J. Phys. Chem. **88**, 3682 (1984).
[67] U. M. B. Marconi, J. Wiechen, and F. Forstmann, Chem. Phys. Lett. **107**, 314 (1984).
[68] C. W. Outhwaite and L. B. Bhuiyan, J. Chem. Phys. **84**, 3461 (1986).
[69] M. Valiskó, D. Henderson, and D. Boda, J. Phys. Chem. B **108**, 16548 (2004).
[70] D. Gillespie, M. Valiskó, and D. Boda, J. Phys.: Condens. Matter **17**, 6609 (2005).
[71] M. Valiskó, D. Boda, and D. Gillespie, J. Phys. Chem. C **111**, 15575 (2007).
[72] A. A. Chialvo and J. M. Simonson, J. Phys. Chem. C **112**, 19521 (2008).
[73] S. L. Carnie and G. M. Torrie, Adv. Chem. Phys. **56**, 141 (1984).
[74] L. Bari Bhuiyan and C. W. Outhwaite, Phys. Chem. Chem. Phys. **6**, 3467 (2004).
[75] J. Yu, G. E. Aguilar-Pineda, A. Antillón, S.-H. Dong, and M. Lozada-Cassou, J. Colloid Interface Sci. **295**, 124 (2006).
[76] R. Messina, J. Chem. Phys. **127**, 214901 (2007).
[77] G. M. Torrie, J. P. Valleau, and C. W. Outhwaite, J. Chem. Phys. **81**, 6296 (1984).
[78] D. A. McQuarrie, *Statistical Mechanics* (Harper, New York, 1976).
[79] J. P. Hansen and I. R. McDonald, *Theory of Simple Liquids* (Academic, London, 1986).
[80] L. Blum, Mol. Phys. **30**, 1529 (1975).
[81] L. Blum and J. S. Hoye, J. Phys. Chem. **81**, 1311 (1977).
[82] K. Hiroike, Mol. Phys. **33**, 1195 (1977).
[83] R. J. Hunter, *Zeta Potential in Colloid Science* (Academic, New York, 1981).
[84] F. Fenell-Evans and H. Wennerström, *The Colloidal Domain: Where Physics, Chemistry, Biology and Technology Meet* (Wiley-VCH, New York, 1994).
[85] E. González-Tovar, M. Lozada-Cassou, and W. Olivares, J. Chem. Phys. **94**, 2219 (1991).
[86] E. González-Tovar, M. Lozada-Cassou, M. M.-N. L. Mier-y Terán, and L. Degrève, in *Lectures in Thermodynamics and Statistical Mechanics: Proceedings of the XXII Winter Meeting on Statistical Physics*, edited by M. L. de Haro and C. Varea (World Scientific, Singapore, 1993).
[87] Q. R. Huang, P. L. Dubin, C. N. Moorefield, and G. R. Newkome, J. Phys. Chem. B **104**, 898 (2000).
[88] V. Tohver, J. E. Smay, P. V. Braun, and J. A. Lewis, Proc. Natl. Acad. Sci. U.S.A. **98**, 8950 (2001).
[89] I. Popa, M. Trulsson, G. Papastavrou, M. Borkovec, and B. Jönsson, Langmuir **25**, 12435 (2009).
[90] D. Gorwyn and G. T. Barnes, Langmuir **6**, 222 (1990).

[91] N. Cuvillier and F. Rondelez, Thin Solid Films **327–329**, 19 (1998).
[92] J. N. Israelachvili, *Intermolecular and Surface Forces*, 2nd ed. (Academic, London, 2002).
[93] M. P. Allen and D. J. Tildesley, *Computer Simulation of Liquids* (Oxford University Press, New York, 1989).
[94] D. Frenkel and B. Smit, *Understanding Molecular Simulation* (Academic, London, 2002).
[95] L. Gierst, L. Vandenberghen, E. Nicolas, and A. Fraboni, J. Electrochem. Soc. **113**, 1025 (1966).
[96] Y. G. Bérubé and P. L. de Bruyn, J. Colloid Interface Sci. **28**, 92 (1968).
[97] S. H. Behrens, D. I. Christl, R. Emmerzael, P. Schurtenberger, and M. Borkovec, Langmuir **16**, 2566 (2000).